

**Treatment for myocardial infarction: *in vivo* evaluation of curcumin-loaded PEGylated-GQDs nanoparticles**

**Running title:** the effects of Cur-PEG-GQDs on MI

Farzaneh Rostamzadeh<sup>1</sup> (PhD), Saeideh Jafarinejad-Farsangi<sup>2\*</sup> (PhD), Zeinab Ansari-Asl<sup>3\*</sup> (PhD), Mitra Shadkam Farrokhi<sup>4</sup> (MSc), Elham Jafari<sup>5</sup> (MD)

1. Physiology Research Center, Institute of Neuropharmacology, Kerman University of Medical Sciences, Kerman, Iran
2. Cardiovascular Research Center, Institute of Basic and Clinical Physiology Sciences, Kerman University of Medical Sciences, Kerman, Iran
3. Department of Chemistry, Faculty of Science, Shahid Chamran University of Ahvaz, Ahvaz, Iran
4. Endocrinology and Metabolism Research Center, Institute of Basic and Clinical Physiology Sciences, Kerman University of Medical Sciences, Kerman, Iran.
5. Pathology and Stem Cell Research Center, Kerman University of Medical Sciences, Kerman, Iran

**Corresponding Author:** Saeideh Jafarinejad-Farsangi\*, Physiology Research Center, Boulevard Jihad, Ebne-Sina Avenue, Postcode: 7619813159, Kerman, Iran. Tel.: +983432236839; fax: +98 343 2264097. Email: [s.jafarinejad@kmu.ac.ir](mailto:s.jafarinejad@kmu.ac.ir); Zeinab Ansari-Asl\*, Email: [z.ansari@scu.ac.ir](mailto:z.ansari@scu.ac.ir);

Chemistry Department. Shahid Chamran University of Ahvaz Ahvaz, Iran. *Postal code*: 61357-43311

**Funding:** This work was supported by grants from the Vice-Chancellor for Research and Technology at Kerman University of Medical Sciences, Kerman, Iran (grant No. IR.KMU.REC.98000918).

The authors have no conflict of interest. The authors have no relevant financial or non-financial interests to disclose

## Abstract

Curcumin (Cur) has been suggested as a complementary treatment for cardiovascular diseases. Its efficiency, however, is modest due to poor biocompatibility. This study examined the effects of curcumin loaded on polyethylene glycol-graphene quantum dots (Cur-PEG-GQDs) on hemodynamic and cardiac function in rats with myocardial infarction (MI). The study groups included control, MI, MI+Cur-3, MI+Cur-7, MI+Cur-15, MI+PEG-GQDs-5, MI+PEG-GQDs-10, MI+Cur-PEG-GQDs-5, MI+Cur-PEG-GQDs-10. MI was established by left anterior descending artery ligation. Two weeks following intraperitoneal administration of vehicle, Cur, PEG-GQDs, and Cur-PEG-GQDs, blood pressure and heart contractility indices were measured. Triphenyl tetrazolium chloride, colorimetry, and clinical laboratory methods were used to measure the infarct size, the oxidant and antioxidant content, and the kidney and liver function parameters, respectively. In the MI animals, Cur-7, PEG-GQDs-10, Cur-PEG-GQDs-5, and Cur-PEG-GQDs-10 recovered SBP, DBP, LVSP, and  $\pm$  dp/dt max disturbances and reduced myocardial infarct size, fibrosis, and LVEDP. Curcumin lowered antioxidant markers and

elevated one oxidant marker in the heart in a dose-dependent manner. Although Cur-PEG-GQDs-5 and -10 reduced curcumin's oxidative stress effects, the SOD, GPX, and TAC levels were significantly lower in Cur-PEG-GQDs-5 and -10 groups compared to the MI group. MDA levels were lower in Cur-PEG-GQDs-5 and -10 groups compared to the Cur-3, -7, and -15 groups. GSH/GSSG ratio improved in the groups treated by Cur-7, PEG-GQDs-10, Cur-PEG-GQDs-5, and Cur-PEG-GQDs-10. The findings indicated that Cur-PEG-GQDs mitigated MI-induced cardiac dysfunction. However, due to the increase in oxidative stress in the heart, nonclassic mechanisms may be involved in the beneficial effect of Cur-PEG-GQDs on MI-induced cardiac dysfunction.

**Keywords:** myocardial infarction, oxidative stress, curcumin, curcumin-polyethylene glycol-graphene quantum dot, nanoparticles

## Introduction

Cardiovascular diseases (CVDs) are relatively common and are one of the leading causes of disability and mortality worldwide.<sup>1</sup> The World Health Organization attributes (WHO) 32% of all-cause mortality to cardiovascular events. Among them, ischemic diseases, such as myocardial infarction (MI) and strokes, are responsible for 85% of deaths.<sup>2</sup> It is vital that harmful consequences of MI, such as fibrosis, scarring, cardiac remodeling, and heart failure, be prevented with appropriate and timely interventions to protect intact and live cells.<sup>3</sup> Using herbal agents as a complementary therapy is one of the best potential interventions.<sup>4,5</sup>

Curcumin, the main component of *Curcuma longa* (turmeric), is used for medical purposes and as food flavoring.<sup>6</sup> The curative effects of curcumin are mainly attributed to its antioxidant, anti-inflammatory, and anti-apoptotic properties.<sup>7-9</sup> The positive effects of curcumin on CVDs have been also reported.<sup>9,10</sup> Curcumin inhibits left ventricular hypertrophy and heart failure induced

by hypertension and MI. Studies have revealed that curcumin has a protective and therapeutic impact on diabetic cardiomyopathy, arrhythmias, and ischemic reperfusion injuries.<sup>6,9,11</sup> The protective effects of curcumin against MI are similar to enalapril. It also ameliorates atherosclerosis and vascular dysfunction.<sup>5</sup>

Curcumin has positive pharmacological effects and is safe to use in clinical studies, but due to its low water solubility and rapid metabolism in the liver, it has poor distribution and bioavailability.<sup>12</sup> However, new technologies may be able to eliminate this limitation. Due to their potential capacity to carry and deliver drugs to target tissues, nanomaterials may be able to solve problems with distribution and bioavailability.<sup>13,14</sup> Nanographenes, biocompatible components with remarkable optical, thermal, and electrochemical properties, can be loaded with drugs.<sup>14,15</sup> Among graphene derivatives, graphene quantum dots (GQDs), graphene sheets with 1–2 layers, have outstanding physiological stability.<sup>16,17</sup> They have potential implications in bioimaging and biomedicine as biosensors<sup>18</sup> and drug carriers.<sup>19</sup> The beneficial effects of polyethylene glycol-graphene quantum dots (PEG-GQDs) on MI injuries through oxidative stress reduction have been demonstrated.<sup>20</sup> Considering their physicochemical properties, small size, various functional groups (epoxy, hydroxyl, and carboxyl), and extensive surface, they are excellent candidates for drug loading and delivery to particular anatomical regions in the body.<sup>21</sup> It has been demonstrated that GQDs release loaded drugs in a controlled manner.<sup>22,23</sup>

Oxidative stress causes ischemia-reperfusion injuries and cardiac dysfunction following MI.<sup>24,25</sup> The apoptosis, necrosis, hypertrophy, and heart remodeling caused by MI have been explained by the excessive production of reactive oxygen species (ROS).<sup>26</sup> It has been demonstrated that curcumin alters oxidant and antioxidant content.<sup>6,27,28</sup> Curcumin protects the heart against



harmful conditions by augmenting superoxide dismutase (SOD) and catalase production and reducing ROS content.<sup>8,29</sup>

Considering the rapid metabolism of curcumin, we assumed that loading it on PEG-GQDs could increase its bioavailability and tissue distribution. Some et al. reported that curcumin loaded on graphene nanoparticles, including graphene quantum dots, has better anticancer activity than free curcumin.<sup>30</sup> The goal of the current study was to examine the effects of free curcumin and curcumin loaded on PEG-GQDs on MI-related complications and heart-related levels of malondialdehyde (MDA), SOD, glutathione peroxidase (GPX), total antioxidant capacity (TAC), and glutathione (GSH) to glutathione disulfide (GSSG) ratio in MI-prone rats.

## **Material and methods**

### **Materials**

The Ethics Committee of Kerman University of Medical Sciences approved the experimental protocol (ethics code IR.KMU.REC.1399.099). Wistar rats were obtained from the Kerman University of Medical Science. The animals were kept in conventional conditions (12 hours of light and 12 hours of darkness) with free water and normal food access. MDA (CAT No: ZB-MDA96), SOD (CAT No. ZB-SOD-96A), and GPX (CAT No : ZB-GPX-A96) assay kits were purchased from ZellBio GmbH (Germany). GSH and GSSG (CAT: NS-15087) were obtained from Navandsalamat. Iran. TAC (Cat No. NX 2332) kit was obtained from Randox (UK). Serum alanine aminotransferase (ALT), aspartate aminotransferase (AST), alkaline phosphatase (ALP), urea, and creatinine were tested using assay kits from Parsazemon, Iran. Triphenyl tetrazolium chloride (TTC) (CAT No: T8877) was acquired from Sigma, UK.

## Methods

The experimental groups (12 rats in each group) included sham as control (CTL), myocardial infarction (MI), MI+PEG-GQDs-5, MI+PEG-GQDs-10, MI+Cur-3, MI+Cur-7, MI+Cur-15, MI+Cur-PEG-GQDs-5, and MI+Cur-PEG-GQDs-10. Seven rats in each group were used to test the hemodynamic, cardiac function, heart contractility, and biochemical factors. The size of the infarcted area was measured in the five remaining animals.

### Synthesis and characterization of GQDs, PEG-GQDs, and Cur-PEG-GQDs

To prepare GQDs, 1g citric acid was heated and stirred in an oil bath at 200 °C until it turned a yellowish-orange in color. The obtained product was treated with NaOH to adjust the pH to 7.<sup>31</sup> The purification of the as-fabricated GQDs in distilled water was performed for 48 hours through a dialysis membrane (1 kDa). After purification, water was removed by freeze-drying, and finally, the GQDs were dissolved in ethanol (500 mg mL<sup>-1</sup>).

PEG-GQDs was conducted using a 1-ethyl-3-(3-dimethylamino propyl)-carbodiimide (EDC) activator. EDC (50 mM) was added to 0.2 mg mL<sup>-1</sup> of GQDs in a phosphate buffer (50 mM, pH 5.5), stirred for an hour to obtain a homogenous solution, and stirred for three more hours after adding PEG (2000 N, Sigma). The prepared PEG-GQDs were purified by dialysis (3 kDa).<sup>32</sup>

A noncovalent functionalization technique was used to attach curcumin to the PEG-GQDs. PEG-GQDs (0.05 mg mL<sup>-1</sup>) were combined with 0.5 ml curcumin (2.5 mM in dimethyl sulfoxide (DMSO)) in 5 ml water. The mixture was blended at room temperature in a dark location for 24 hours. The excessive curcumin was removed by centrifugation. The supernatant was dialyzed through a 1 kDa bag for 48 hours, and after freeze-drying to remove any leftover undissolved

free curcumin, the remaining Cur-PEG-GQDs were kept at 4 °C. The amount of loaded curcumin was evaluated by its absorbance at 422 nm wavelength (UV-Vis spectroscopy).<sup>33</sup>

The characterization of GQDs, PEG-GQDs, and Cur-PEG-GQDs was performed by ultraviolet-visible spectroscopy (UV-Vis), Fourier transforms infrared spectroscopy (FT-IR), transmission electron microscopy (TEM) images, and dynamic light scattering (DLS) methods.

### **Curcumin release from Cur-PEG-GQDs**

Curcumin release from Cur-PEG-GQDs was evaluated in phosphate-buffered saline (PBS) at pH 7.4.<sup>34</sup> The Cur-PEG-GQDs were dialyzed in a dialysis sac (1 kDa cut off), and the released curcumin was measured in the medium at different time points using UV-Vis spectroscopy. All procedures were performed in triplicate at room temperature.<sup>35</sup>

### **Induction of myocardial infarction**

The left anterior descending (LAD) coronary artery was occluded for induction of MI, as described in a previous study.<sup>36</sup> Animals were kept under mechanical ventilation during the procedures under anesthesia (ketamine/xylazine 80/10 mg kg<sup>-1</sup>). Following an incision in the fourth intercostal space on the left side, the pericardium was opened, and the LAD was ligated using a 6/0 silk suture 2 mm below its origin. After LAD ligation, the appearance of the at-risk area changed, and the ST segment in ECG elevated. In the sham group (CTL), all the steps mentioned above were performed except for the ligation of the LAD.

### **Treatment with Cur, PEG-GQDs, and Cur-PEG-GQDs**

Curcumin was injected intraperitoneally (IP) at three doses of 3, 7, and 15 mg kg<sup>-1</sup> every other day for two weeks. The 15 mg kg<sup>-1</sup> curcumin dose was chosen according to a previous study.<sup>37</sup>

However, the lower doses (3 and 7 mg kg<sup>-1</sup>) were also used to determine ineffective doses. The previous study showed that PEG-GQDs have no curative effects at 5 mg kg<sup>-1</sup> but are effective at 10 mg kg<sup>-1</sup> on MI.<sup>20</sup> Therefore, in this study, curcumin was loaded on PEG-GQDs at 5 mg kg<sup>-1</sup> (ineffective dose) and 10 mg kg<sup>-1</sup> (effective dose) to produce Cur-PEG-GQDs. Each mg of PEG-GQDs loads 0.003 mg of curcumin, so Cur-PEG-GQDs at the dose of 10 mg kg<sup>-1</sup> has twice the concentration of Cur. PEG-GQDs and Cur-PEG-GQDs were administered every other day for 14 days, as was curcumin (Figure 1). As a vehicle of curcumin and Cur-PEG-GQDs, DMSO diluted in distilled water was injected in the CTL and MI groups.

### **Recording of hemodynamic parameters**

Hemodynamic parameters were recorded under anesthesia induced with sodium thiopental (50 mg kg<sup>-1</sup>). The systolic blood pressure (SBP), diastolic blood pressure (DBP), and heart rate (HR) were recorded by a femoral artery catheter filled with heparin saline. Cardiac function and heart contractility indices, including left ventricular systolic pressure (LVSP), left ventricular end-diastolic pressure (LVEDP), maximum rate of increase in left ventricular pressure during systole (+dp/dt max), and maximum rate of decrease in left ventricular pressure during diastole (-dp/dt max) were recorded by another catheter inserted into the left ventricle (LV).<sup>38</sup> The cannulas were connected to pressure transducers and then linked to a PowerLab system (8-channel; ADInstruments, Australia). The animals were ventilated through a tracheal cannula if necessary.

### **Preparation of heart tissue and serum**

After recording cardiac function indices and hemodynamic parameters, blood was collected under deep anesthesia and kept at room temperature for 2 hours. Then, the serum was separated

from the clotted blood and centrifuged at 4000 rpm for 15 minutes. The septum and left ventricle (LV) were carefully removed from the heart and frozen at -80 °C. Biochemical variables were measured using heart tissue samples from the peri-infarcted region.

### **Measurement of infarct area and fibrosis**

The hearts were kept at -20 °C for 1 to 2 hours. After that, 3-mm-thick slices were dyed for 20 minutes at 37 °C with 1% TTC in PBS. Finally, the slices were immersed in 10% formaldehyde for 10 minutes. ImageJ software 27 was used to calculate the infarcted area (pale) ratio to the total LV area. For fibrosis assessment, sections of the left ventricle were fixed in 10% buffered formalin (pH 7.4), embedded in paraffin, cut into 5- $\mu$ m-thick sections, and stained with Masson's trichrome. A pathologist blind to the group belonged to examined the sections under a microscope. The percentage of fibrosis was calculated by Image j software.<sup>20</sup>

### **Measurement of oxidative stress indices**

The SOD activity was determined using the directions of the related kit. In brief, cardiac tissue (100 mg) was homogenized in a solution of 100 mM PBS and then centrifuged for 20 minutes at 4 °C at 4000–6000 rpm. SOD activity was measured using 50 $\mu$ l of the supernatant by colorimetric method. The absorbance density was measured at 420 nm. GPX activity was assessed with 100 mg of heart tissue homogenized in 200  $\mu$ l of the assay buffer. The homogenate was centrifuged for 15 minutes at 10000 x g at 4 °C. Then, the supernatant was separated to determine the activity of GPX. MDA was measured using the thiobarbituric acid reaction in 100 mg of homogenized tissue that had been lysed in a KCl (1.5%) solution and centrifuged at 1200 rpm (10 min). TAC levels were measured according to kit instructions. For measuring the levels of GSH, GSSG, and

their ratio, 50 mg heart tissue was homogenized in lysing buffer and then centrifuged at 9000 rpm for 15 min. The supernatant was used to measure GSH and GSSG according to the instructions of the associated kit.

### **Assessment of treatment side effects on liver and kidney function**

Side effects of curcumin and Cur-PEG-GQDs on the kidneys and liver were determined by measuring the serum levels of ALT, AST, ALK, creatinine, and urea via the photometric method (Selectra E, Japan).

### **Statistical analysis**

The data in the table and figures is presented as mean  $\pm$  standard error of the mean (SEM). The Shapiro-Wilk test was used to evaluate the normal distribution of data. One-way analysis of variance (ANOVA) was used for comparisons among different groups, and in case of significance, pairwise comparisons were conducted by Tukey's post hoc test.  $P$  values  $< 0.05$  were considered significant.

## **Results**

### **Characterization of GQDs, GQDs, and Cur-PEG-GQDs**

The GQDs, PEG-GQDs, and Cur-PEG-GQDs functional groups were investigated using FT-IR spectroscopy (Figure 2A). FT-IR studies confirmed the presence of various oxygen-containing groups on the as-obtained GQDs. These functional groups caused the hydrophilicity of the GQDs and stability in aqueous solutions. The stretching vibration peak of the O-H and C-H groups were exhibited at  $3334\text{ cm}^{-1}$  and  $2932\text{ cm}^{-1}$ , respectively. The characteristic peaks at  $1720\text{ cm}^{-1}$ ,  $1616$

$\text{cm}^{-1}$ ,  $1228\text{ cm}^{-1}$ , and  $1033\text{ cm}^{-1}$  correspond to the C=O, C=C, C-OH, and C-O-C, respectively. The attachment of the PEG onto GQDs was confirmed by FT-IR spectroscopy. As shown in the FT-IR spectrum of the PEG-GQDs, the characteristic peaks of PEG are exhibited at  $2879\text{ cm}^{-1}$  and  $1105\text{ cm}^{-1}$  owing to the stretching vibrations of the C-H and C-O-C groups, respectively. For Cur-PEG-GQDs, bands observed at  $3512\text{ cm}^{-1}$  ( $\nu(\text{O}-\text{H})$ ),  $1626\text{ cm}^{-1}$  ( $\nu(\text{C}=\text{C})$ ),  $1510\text{ cm}^{-1}$  ( $\nu(\text{C}=\text{O})$  and  $\nu(\text{C}=\text{C})$ ),  $1430\text{ cm}^{-1}$  ( $\nu(\text{C}-\text{H})$ ),  $1282\text{ cm}^{-1}$  ( $\nu(\text{C}-\text{O})$ ), and  $1028\text{ cm}^{-1}$  ( $\nu(\text{C}-\text{O}-\text{C})$ ) are attributed to curcumin. The UV-vis spectra of the GQDs, PEG-GQDs, Cur, and Cur-PEG-GQDs were recorded in DMSO solutions (Figure 2 B). A strong absorption around 235 nm corresponds to the  $\pi-\pi^*$  transitions. In the pure Cur UV-vis spectrum, a band associated with the  $\pi-\pi^*$  shifts are detected at around 425 nm. The appearance of this peak confirms the preparation of the Cur-PEG-GQDs. Figures 2 C, D, and E exhibit the TEM images of the GQDs, PEG-GQDs, and Cur-PEG-GQDs, respectively, which show spherical morphology similar to the pristine GQDs. The GQDs, PEG-GQDs, and Cur-PEG-GQDs were relatively monodispersed with diameters around 15 nm, 5 nm, and 17 nm, respectively. DLS method was used to study the size distribution of the Cur-PEG-GQDs; the obtained results confirm narrow size distribution for the as-fabricated materials (Figure 2 F). The average diameter of Cur-GQD-PEG particles obtained from the DLS was around 14.7 nm. According to Figure 3G, curcumin release reaches 60% five hours after injection.

Collectively, the water-soluble and uniform-sized GQDs were successfully modified by the PEG and Cur, respectively. The unique photoluminescence and narrow size distributions of well-fabricated PEG-GQDs and Cur-PEG-GQDs nanocomposites are crucial for biological applications. The PEG is used to increase the hydrophilic properties of the surfaces and colloidal stability.

### **The effects of treatments on body weight, lung, heart, and left ventricular weight/body weight ratio, infarct size, and fibrosis**

Bodyweight, heart weight/body weight, and left ventricular weight/body weight ratio were not different among the studied groups (Table 1). The MI group's lung weight/body weight ratio insignificantly increased compared to the CTL group, but it decreased after treatment with 5 and 10 mg kg<sup>-1</sup> of Cur-PEG-GQDs ( $P < 0.05$ ).

The size of the infarct area in the heart of the MI group was 42%. Curcumin at the dose of 7 mg kg<sup>-1</sup> significantly decreased the infarct area ( $P < 0.001$ ). However, curcumin at low and high doses (3 and 15 mg kg<sup>-1</sup>) did not significantly affect the size of the infarct area. In contrast to PEG-GQDs-5, which did not affect infarct size, PEG-GQDs-10 significantly reduced the infarct size ( $P < 0.001$ ). Cur-PEG-GQDs-5 and Cur-PEG-GQDs-10 also significantly decreased the infarct size compared to the MI group ( $P < 0.001$ ) (Figure 3A, B). The percentage of fibrosis in the MI group was 23%. Curcumin was able to reduce fibrosis at 7 mg kg<sup>-1</sup> by 11.3% ( $P < 0.01$ ). PEG-GQDs-10, Cur-PEG-GQDs-5, and Cur-PEG-GQDs-10 also significantly decreased the fibrosis compared to the MI group ( $P < 0.05$ ) (Figure 4A, B).

In sum, these data suggested that curcumin and Cur-PEG-GQDs alleviated cardiac injuries and fibrosis that had occurred during MI in rats.

### **Effect of treatments on hemodynamic parameters and cardiac index**

SBP ( $P < 0.001$ ) and DBP ( $P < 0.05$ ) decreased in the MI group compared to the CTL group. Curcumin at the dose of 7 mg kg<sup>-1</sup> restored the reduction of SBP and DBP in the MI group. However, the low and high doses of curcumin did not significantly affect SBP and DBP changes (Figure 5A, B). PEG-GQDs-5 and PEG-GQDs-10 were not able to inhibit the effects of MI on



SBP and DBP. However, Cur-PEG-GQDs-5 increased SBP compared with the MI and PEG-GQDs-5 groups ( $P < 0.05$ ). PEG-GQDs-10 also increased the SBP ( $P < 0.01$ ) compared to the MI group. No change in HR was observed in any group (Figure 5C). There was a decrease in LVSP in the MI group ( $P < 0.001$ ). At doses of 7 ( $P < 0.001$ ) and 15 mg/kg ( $P < 0.05$ ), but not at dose 3, Curcumin increased LVSP in comparison with the MI group. PEG-GQDs-10, Cur-PEG-GQDs-5, and Cur-PEG-GQDs-10 significantly restored LVSP to normal levels ( $P < 0.001$ ). Cur-PEG-GQDs-5 also significantly increased LVSP compared to PEG-GQDs-5 ( $P < 0.001$ ) (Figure 6A). LVEDP increased in the MI group ( $P < 0.05$ ). At doses 3 ( $P < 0.01$ ), 7 ( $P < 0.05$ ), and 15 ( $P < 0.01$ ), curcumin significantly reduced LVEDP compared with the MI group. PEG-GQDs-5 and Cur-PEG-GQDs-5 had no impact on LVEDP. However, LVEDP dropped significantly in the animals that received PEG-GQDs-10 and Cur-PEG-GQDs-10 ( $P < 0.001$ ) (Figure 6B).

+ dp/dt max and -dp/dt max were significantly lower in the MI group ( $P < 0.001$ ). They were increased by curcumin at the dose of 7 mg kg<sup>-1</sup>. The treatment of PEG-GQDs-5 could not compensate for the decline of +max dp/dt and -max dp/dt, but Cur-PEG-GQDs-5 significantly increased +dp/dt max and -dp/dt max compared to the MI group. PEG-GQDs-10 and Cur-PEG-GQDs-10 alleviated the impact of MI on the indices mentioned above ( $P < 0.001$ ) (Figure 6C, D).

These results showed curcumin, and Cur-PEG-GQDs exerted beneficial effects on hemodynamic parameters, cardiac function, and contractility in hearts of rats with MI.

### **Effect of treatments on oxidative stress and liver and kidney function tests**

The results showed that curcumin increased MDA levels in the MI group at all doses. MDA levels were higher in animals that took curcumin at the dose of 15 mg kg<sup>-1</sup> compared to those who took the lower doses. When curcumin was loaded on PEG-GQDs, MDA levels significantly decreased compared with the curcumin groups ( $P < 0.01$ ) (Figure 7A). TAC and GPX levels were lower in the MI group compared to the CTL group ( $P < 0.05$ ). Curcumin at all doses decreased GPX, SOD, and TAC levels compared to the CTL and MI groups ( $P < 0.05$ ) ( $P < 0.001$ ). These effects were dose-dependent: At the highest dose, 15 mg kg<sup>-1</sup>, the effect was more remarkable than at lower doses ( $P < 0.01$ ). PEG-GQDs-10 significantly increased GPX ( $P < 0.05$ ) and TAC ( $P < 0.001$ ). However, in the rats treated with Cur-PEG-GQDs-5 and -10, SOD, TAC, and GPX decreased compared to the CTL and MI groups. Loading Cur on PEG-GQDs-5 and -10 reduced the above-mentioned antioxidant levels compared to PEG-GQDs-5 ( $P < 0.05$ ) and PEG-GQDs-10 ( $P < 0.01$ ), respectively (Figure 7B-D).

The GSH levels and ratio of reduced to oxidized glutathione (GSH/GSSG), an indicator of cellular toxicity, decreased in the MI group compared to the CTL group ( $P < 0.001$ ) (Figure 8). In addition, the GSSG level increased in the heart with MI. Cur 7 and 15, PEG-GQDs-5 and -10, and Cur-PEG-GQDs-5 and -10 partly restored the GSH level and GSH/GSSG ratio ( $P < 0.05$  to 0.001). GSSH levels were lower in the Cur 15, PEG-GQDs-10, and Cur-PEG-GQDs-5 and -10 groups than in the MI group ( $P < 0.05$  to  $P < 0.01$ ) (Figure 8).

ALP increased in groups that received curcumin at 3 and 15 mg kg<sup>-1</sup>. Cur-7 decreased levels of ALT and AST in the heart ( $P < 0.05$ ). AST levels in the heart also decreased in the Cur-PEG-GQDs group (Figure 9). The amount of urea and creatinine was not different among different groups (Figure 10).

The results indicated that the curcumin loaded on PEG-GQDs mitigated the effects of free curcumin on oxidative stress, probably due to its doses which are remarkably lower than free curcumin.

## Discussion

The findings of this study showed that curcumin improved left ventricular efficiency in a dose-dependent manner, indicated by the increase in the  $\pm dp/dt$  max and LVSP and the decrease in LVEDP and myocardial infarct size and fibrosis. Curcumin also restored the reduction of SBP and DBP, which had occurred in animals with MI. Curcumin had no positive effects on cardiac function at higher doses, probably due to extra oxidative stress production. Although the amount of curcumin loaded on PEG-GQDs was much lower than the ineffective low-dose free curcumin, it also improved myocardial efficiency, modified blood pressure, and decreased myocardial infarct size and fibrosis. This demonstrated the excellent efficiency and performance of the drug delivery to the heart by PEG-GQDs.

In various experimental and clinical studies, the beneficial effects of curcumin on different CVDs have been demonstrated.<sup>39,5</sup> The oral intake of curcumin at the dose of 150 mg kg<sup>-1</sup> per day significantly attenuates oxidative stress and improves cardiac dysfunction induced by ischemic-reperfusion injuries.<sup>39</sup> Another study also suggested that curcumin pretreatment protects the heart from deleterious consequences of isoproterenol-induced cardiac damage.<sup>29</sup> The present study results also indicated that curcumin at 7 mg kg<sup>-1</sup> improved cardiac function and restored blood pressure in rats with MI. However, it seems the beneficial impacts of curcumin are determined by its dose, as positive effects diminished at high doses.

The reduction of the levels of GPx, TAC, SOD, and the ratio of GSH/GSSG highlighted the role of oxidative stress in the harmful consequences of myocardial infarction. The antioxidative properties of curcumin have been recognized for years. Many studies have shown that some of the valuable functions of curcumin are due to the regulation of oxidative stress.<sup>5</sup> However, our results indicated that curcumin increased MDA, a marker for oxidant production, and decreased antioxidant capacity (SOD, GPX, and TAC) in the heart with MI, even in the ineffective low dose (3 mg kg<sup>-1</sup>). The rise in the ratio of GSH/GSSG in the effective dose of curcumin (7 mg kg<sup>-1</sup>) probably diminished the deleterious effects of curcumin on oxidative stress by improvement of the redox equilibrium.

The severe disturbance in the oxidant/antioxidant equilibrium, so that the increase in the ratio of GSH/GSSH could not compensate for it, could explain the diminished therapeutic impact of Cur-15, which was significantly higher at the dose of 15 mg kg<sup>-1</sup> compared to other doses (3 and 7). The level of oxidative stress is probably essential to prevent its harmful effects.

Many discrepancies have been observed regarding the regulatory effect of curcumin on oxidant/antioxidant balance.<sup>8,40,41</sup> Besides the antioxidative properties of curcumin, there is ample evidence regarding the pro-oxidant effects of curcumin found in our study. Curcumin promotes apoptosis by augmentation of ROS production in tumor cells.<sup>41</sup> It has also been revealed that curcumin increases ROS-related apoptosis in cardiomyocytes.<sup>7</sup> Reports indicate that orally administrated curcumin acts as a pro-oxidant and does not improve the deleterious effects of isoproterenol-induced cardiac ischemia at higher doses.<sup>42</sup>

Although there are some assumptions about curcumin's stimulation of ROS production, the exact mechanisms are unknown. It has been suggested that the pro-oxidative or antioxidative

properties of curcumin are related to the type of cells, drug administration route, and concentration.<sup>43</sup>

Due to curcumin's high metabolism and hydrophobic features, its bioavailability is very poor. Some solutions to overcome this limitation include loading it on nanoparticles or inserting them into liposomes.<sup>11,44</sup> In this study, curcumin was loaded on PEG-GQDs, a graphene derivative with known biological and medical functions.<sup>14</sup> PEG-GQDs have an excellent capacity to carry drugs such as doxorubicin.<sup>22</sup> As expected, loading curcumin on PEG-GQDs increased its bioavailability and efficiency. The findings showed that Cur-PEG-GQDs-5, which is the outcome of loading curcumin onto the ineffective dose of PEG-GQDs ( $5 \text{ mg kg}^{-1}$ ), attenuated the harmful results of MI. The content of curcumin loaded on PEG-GQDs was 0.003 mg of curcumin per 1 mg of PEG-GQDs, which is less than the ineffective dose of free curcumin ( $3 \text{ mg kg}^{-1}$ ). There is a probability that nanoparticles increase the accessibility of the heart to curcumin. PEG-GQDs-10 has curative effects on cardiac function and normalized left ventricular contractility probably due to the antioxidative effects of PEG-GQDs (Figure 7). Similar to PEG-GQDs-10, Cur-PEG-GQDs-10 recovered cardiac efficiency and reduced the infarcted area size. This similarity was, probably due to the maximum positive responses achieved by the dose of GOD-PEG-10 on cardiac injuries. Since contrary to PEG-GQDs-10, Cur-PEG-GQDs-10 restored the reduction in SBP and DBP, the modification of these parameters can be attributed to the curcumin loaded on PEG-GQDs-10. Although DBP was restored partly by GOD-PEG 10 and Cur-GOD-PEG 5, its elevation was insignificant. This might be due to GOD-PEG 10 and Cur-GOD-PEG 5 on peripheral resistance since DBP is mainly affected by vascular resistance, while SBP is affected mainly by cardiac output.<sup>45</sup> It has been reported curcumin increases vascular function by improving nitric oxide bioavailability and reducing oxidative stress.<sup>46</sup>

The inhibition of MDA production by Cur-PEG-GQDs suggested that reducing the dose of curcumin by loading it on PEG-GQDs preserves the beneficial effects of curcumin without this disadvantage. In addition, PEG-GQDs and Cur-PEG-GQDs alleviated cardiac oxidative stress by increasing the ratio of GSH/GSSG and improving the redox equilibrium.

Although many studies have demonstrated the safety of curcumin consumption, few studies have examined if curcumin has harmful effects.<sup>43</sup> Therefore, the liver and kidney toxicity of curcumin, PEG-GQDs, and Cur-PEG-GQDs were evaluated in this study. The data indicated that curcumin at doses of 3 and 7 g/kg increased alkaline phosphatase levels. This may result from the impact of curcumin on osteoblasts or intestines.<sup>47</sup> Another study also reported that receiving 0.45 to 3.6 g/day curcumin for one to four months increased serum alkaline phosphatase and lactate dehydrogenase.<sup>48</sup> However, at the effective dose of 7 mg kg<sup>-1</sup>, curcumin recovered the elevated liver enzymes, ALT, and AST to normal values. The elevation of AST and ALT in patients with ST-segment elevation myocardial infarction (STEMI) independently predicts all-cause mortality.<sup>49</sup> However, in the present study, Cur-PEG-GQDs had no detrimental effects on the liver and kidneys since ALP, ALT, AST, urea, and creatinine levels were all within normal limits.

**Conclusion:** The findings indicated that PEG-GQDs have the potential capacity to load and deliver curcumin to the heart. Curcumin loaded on PEG-GQDs has the same positive effects on cardiac function and contractility as free curcumin, even at lower doses. Therefore, by conjugating curcumin with PEG-GQDs, its pharmacological effectiveness and bioavailability may be augmented.

**Conflict of interest:** The authors have no conflict of interest. The authors have no relevant financial or non-financial interests to disclose.

**Authors' contribution:**

FR and SJF designed the research. FR, ZAA, and SJ conducted the experiments. MS analyzed the data. FR, ZAA, and SJF wrote the manuscript. EJ interpreted the fibrosis data. All authors read and approved the final version of the manuscript.

**References**

1. Raphael CE, Roger VL, Sandoval Y, Singh M, Bell M, Lerman A, et al. Incidence, trends, and outcomes of type 2 myocardial infarction in a community cohort. *Circulation*. 2020;141:454–63. doi: 10.1161/CIRCULATIONAHA.119.043100.
2. World Health Organization. Cardiovascular diseases (CVDs). 2021. <https://www.who.int/news-room/fact-sheets/detail/c>.
3. Thygesen K, Alpert JS, Jaffe AS, Chaitman BR, Bax JJ, Morrow DA, et al. Fourth Universal Definition of Myocardial Infarction. *Circulation*. 2018;138:618–651. doi: 10.1161/CIR.0000000000000617.
4. Talman V, Ruskoaho H. Cardiac fibrosis in myocardial infarction—from repair and remodeling to regeneration. *Cell Tissue Res*. 2016;365:563–81. doi: 10.1007/s00441-016-2431-9.
5. Saeidinia A, Keihanian F, Butler AE, Bagheri RK, Atkin SL, Sahebkar A. Curcumin in heart failure: A choice for complementary therapy? *Pharmacol Res*. 2018;131:112-119. doi:10.1016/j.phrs.2018.03.009.

6. Zheng J, Cheng J, Zheng S, Feng Q, Xiao X. Curcumin , A Polyphenolic Curcuminoid With Its Protective Effects and Molecular Mechanisms in Diabetes and Diabetic Cardiomyopathy. *Front Pharmacol*. 2018; 9;9:472. doi:10.3389/fphar.2018.00472.
7. Aggeli KZI. Curcumin induces the apoptotic intrinsic pathway via upregulation of reactive oxygen species and JNKs in H9c2 cardiac myoblasts. *Apoptosis*. 2014;19:958-974. doi:10.1007/s10495-014-0979-y.
8. Nazam Ansari M, Bhandari U, Pillai KK. Protective role of curcumin in myocardial oxidative damage induced by isoproterenol in rats. *Hum Exp Toxicol*. 2007;26:933–8. doi: 10.1177/0960327107085835.
9. Jiang S, Han J, Li T, Xin Z, Ma Z, Di W, et al. Curcumin as a potential protective compound against cardiac diseases. *Pharmacol Res*. 2017;119:373-383. doi: 10.1016/j.phrs.2017.03.001.
10. Yang K, Xu C, Li X, Jiang H. Combination of D942 with curcumin protects cardiomyocytes from ischemic damage through promoting autophagy. *J Cardiovasc Pharmacol Ther*. 2013;18:570–81. doi: 10.1177/1074248413503495.
11. Boarescu PM, Boarescu I, Bocşan IC, Pop RM, Gheban D, Bulboacă AE, et al. Curcumin Nanoparticles Protect against Isoproterenol Induced Myocardial Infarction by Alleviating Myocardial Tissue Oxidative Stress, Electrocardiogram, and Biological Changes. *Molecules*. 2019;24:2802. doi: 10.3390/molecules24152802.
12. Slika L, Patra D. A short review on chemical properties, stability and nano-technological advances for curcumin delivery. *Expert Opin Drug Deliv*. 2020;17:61–75. doi: 10.1080/17425247.2020.1702644.



13. Shah A, Aftab S, Nisar J, Ashiq MN, Iftikhar FJ. Nanocarriers for targeted drug delivery. *J Drug Deliv Sci Technol*. 2021;62:102426. doi:10.1016/j.jddst.2021.102426.
14. Chen F, Gao W, Qiu X, Zhang H, Liu L, Liao P, et al. Frontiers in Laboratory Medicine Graphene quantum dots in biomedical applications : Recent advances and future challenges. *Front Lab Med*. 2018;1:192–9. doi: 10.1016/j.flm.2017.12.006.
15. Tabish TA, Scotton CJ, J Ferguson DC, Lin L, der Veen A van, Lowry S, et al. Biocompatibility and toxicity of graphene quantum dots for potential application in photodynamic therapy. *Nanomedicine*. 2018;13:1923–37. doi: 10.2217/nnm-2018-0018.
16. Mansuriya BD, Altintas Z. Applications of Graphene Quantum Dots in Biomedical Sensors. *Sensors (Basel)*. 2020;20:1072. doi: 10.3390/s20041072.
17. Chong Y, Ma Y, Shen H, Tu X, Zhou X, Xu J, et al. The in vitro and in vivo toxicity of graphene quantum dots. *Biomaterials*. 2014;35:5041–8. doi: 10.1016/j.biomaterials.2014.03.021.
18. Wang K, Li K, Yu B, Shen Y, Cong H. Application of PEGylated graphene quantum dots in cell imaging. *Ferroelectrics*. 2019;547:21–6. doi:10.1080/00150193.2019.1592479.
19. Zheng XT, Ananthanarayanan A, Luo KQ, Chen P. Glowing graphene quantum dots and carbon dots: properties, syntheses, and biological applications. *Small*. 2015;11:1620–1636. doi: 10.1002/smll.201402648.
20. Rostamzadeh F, Shadkam-Farrokhi M, Jafarinejad-Farsangi S, Najafipour H, Ansari-Asl Z, Yeganeh-Hajahmadi M. PEGylated Graphene Quantum Dot Improved Cardiac Function in Rats with Myocardial Infarction: Morphological, Oxidative Stress, and Toxicological

Evidences. *Oxid Med Cell Longev*. 2021;2021:8569225. doi: 10.1155/2021/8569225.

21. Perini G, Palmieri V, Ciasca G, De Spirito M, Papi M. Unravelling the potential of graphene quantum dots in biomedicine and neuroscience. *Int J Mol Sci*. 2020;21:3712. doi: 10.3390/ijms21103712.
22. Zhao C, Song X, Liu Y, Fu Y, Ye L, Wang N, Wang F, Li L, Mohammadniaei M, Zhang M, Zhang Q. Synthesis of graphene quantum dots and their applications in drug delivery. *J. Nanobiotechnology*. 2020;18:142. doi: 10.1186/s12951-020-00698-z.
23. Hosnedlova B, Kepinska M, Fernandez C, Peng Q, Ruttkay-Nedecky B, Milnerowicz H, et al. Carbon nanomaterials for targeted cancer therapy drugs: A critical review. *Chem Rec*. 2019;19(2–3):502–22. doi: 10.1002/tcr.201800038.
24. Wang X, Guo Z, Ding Z, Mehta JL. Inflammation, autophagy, and apoptosis after myocardial infarction. 2018;7(9):e008024. doi: 10.1161/JAHA.117.008024.
25. Peoples JN, Saraf A, Ghazal N, Pham TT, Kwong JQ. Mitochondrial dysfunction and oxidative stress in heart disease. *Exp Mol Med*. 2019;51:1-13. doi: 10.1038/s12276-019-0355-7
26. Takimoto E, Kass DA. Role of oxidative stress in cardiac hypertrophy and remodeling. *Hypertension*. 2007;49:241–8. doi:10.1161/01.HYP.0000254415.31.
27. Wang JL, Wang JJ, Cai ZN, Xu CJ. The effect of curcumin on the differentiation, apoptosis and cell cycle of neural stem cells is mediated through inhibiting autophagy by the modulation of Atg7 and p62. *Int J Mol Med*. 2018;42:2481–8. doi: 10.3892/ijmm.2018.3847.
28. Quiles JL, Huertas JR, Battino M, Mataix J, Ramírez-Tortosa MC. Antioxidant nutrients and adriamycin toxicity. *Toxicology*. 2002;180:79–95. doi: 10.1016/s0300-483x(02)00383-9.
29. Liu R, Zhang HB, Yang J, Wang JR, Liu JX, Li CL. Curcumin alleviates isoproterenol-

induced cardiac hypertrophy and fibrosis through inhibition of autophagy and activation of mTOR. *Eur Rev Med Pharmacol Sci*. 2018;22:7500–8. doi: 10.26355/eurrev\_201811\_16291.

30. Some S, Gwon A-R, Hwang E, Bahn G, Yoon Y, Kim Y, et al. Cancer therapy using ultrahigh hydrophobic drug-loaded graphene derivatives. *Sci Rep*. 2014;4:6314. doi: 10.1038/srep06314.

31. Pimpang P, Sumang R, Choopun S. Effect of concentration of citric acid on size and optical properties of fluorescence graphene quantum dots prepared by tuning carbonization degree. *Chiang Mai J. Sci*. 2018;45:2005-2014.

32. Shen J, Zhu Y, Yang X, Zong J, Zhang J, Li C. One-Pot Hydrothermal Synthesis of Graphene Quantum Dots Surface-Passivated by Polyethylene Glycol and Their Photoelectric Conversion under Near-Infrared Light. *New J Chem*. 2012;36:97-101.

33. Mars A, Hamami M, Bechnak L, Patra D, Raouafi N. Curcumin-graphene quantum dots for dual mode sensing platform: Electrochemical and fluorescence detection of APOe4, responsible of Alzheimer's disease. *Anal Chim Acta*. 2018;1036:141-146. doi: 10.1016/j.aca.2018.06.075.

34. Jafarinejad-Farsangi S, Hashemi MS, Rouholamini SEY, Gharbi S, Ansari-Asl Z, Jafari E, et al. Curcumin loaded on graphene nanosheets induced cell death in mammospheres from MCF-7 and primary breast tumor cells. *Biomed Mater*. 2021;16. doi: 10.1088/1748-605X/ac0400.

35. Danafar H, Salehiabar M, Barsbay M, Rahimi H, Ghaffarlou M, Arbabi Zaboli K, et al. Curcumin delivery by modified biosourced carbon-based nanoparticles. *Nanomedicine (Lond)*. 2022;17:95–105. doi: 10.2217/nnm-2021-0225.

36. Najafipour H, Rostamzadeh F, Yeganeh-Hajahmadi M, Joukar S. Improvement of

Cardiac Function in Rats With Myocardial Infarction by Low-Intensity to Moderate-Intensity Endurance Exercise Is Associated With Normalization of Klotho and SIRT1. *J Cardiovasc Pharmacol.* 2021;77:79–86. doi: 10.1097/FJC.0000000000000935.

37. Hu Y, Mou L, Yang F, Tu H, Lin W. Curcumin attenuates cyclosporine A-induced renal fibrosis by inhibiting hypermethylation of the klotho promoter. *Mol Med Rep.* 2016;14:3229–36. doi: 10.3892/mmr.2016.5601.

38. Rostamzadeh F, Najafipour H, Yeganeh-Hajahmadi M, Esmaili-mahani S, Joukar S, Iranpour M. Heterodimerization of apelin and opioid receptors and cardiac inotropic and lusitropic effects of apelin in 2K1C hypertension: Role of pERK1/2 and PKC. *Life Sci.* 2017;191:24–33. doi: 10.1016/j.lfs.2017.09.044.

39. Wang NP, Wang ZF, Tootle S, Philip T, Zhao ZQ. Curcumin promotes cardiac repair and ameliorates cardiac dysfunction following myocardial infarction. *Br J Pharmacol.* 2012;167:1550–62. doi: 10.1111/j.1476-5381.2012.02109.x.

40. Liu Z, Huang P, Law S, Tian H, Leung W, Xu C. Preventive effect of Curcumin against chemotherapy-induced side-effects. *Front Pharmacol.* 2018;9:1374. doi: 10.3389/fphar.2018.01374.

41. Araveti PB, Srivastava A. Curcumin induced oxidative stress causes autophagy and apoptosis in bovine leucocytes transformed by *Theileria annulata*. *Cell Death Discov.* 2019 ;5:100. doi: 10.1038/s41420-019-0180-8.

42. Broskova Z, Drabikova K, Sotnikova R, Fialova S, Knezl V. Effect of plant polyphenols on ischemia-reperfusion injury of the isolated rat heart and vessels. *Phyther Res.* 2013;27:1018–22. doi: 10.1002/ptr.4825.

43. Burgos-Morón E, Calderón-Montaña JM, Salvador J, Robles A, López-Lázaro M. The

dark side of curcumin. *Int J Cancer*. 2010;126:1771-1775. doi: 10.1002/ijc.24967.

44. Kongkaneramt L, Aiemsun-ang P, Kewsuwan P. Development of curcumin liposome formulations using polyol dilution method. 2016;38:605–10.

45. Pappano AJ, Wier WG. *Cardiovascular Physiology-E-Book*. Elsevier Health Sciences, 2018 Sep 6.

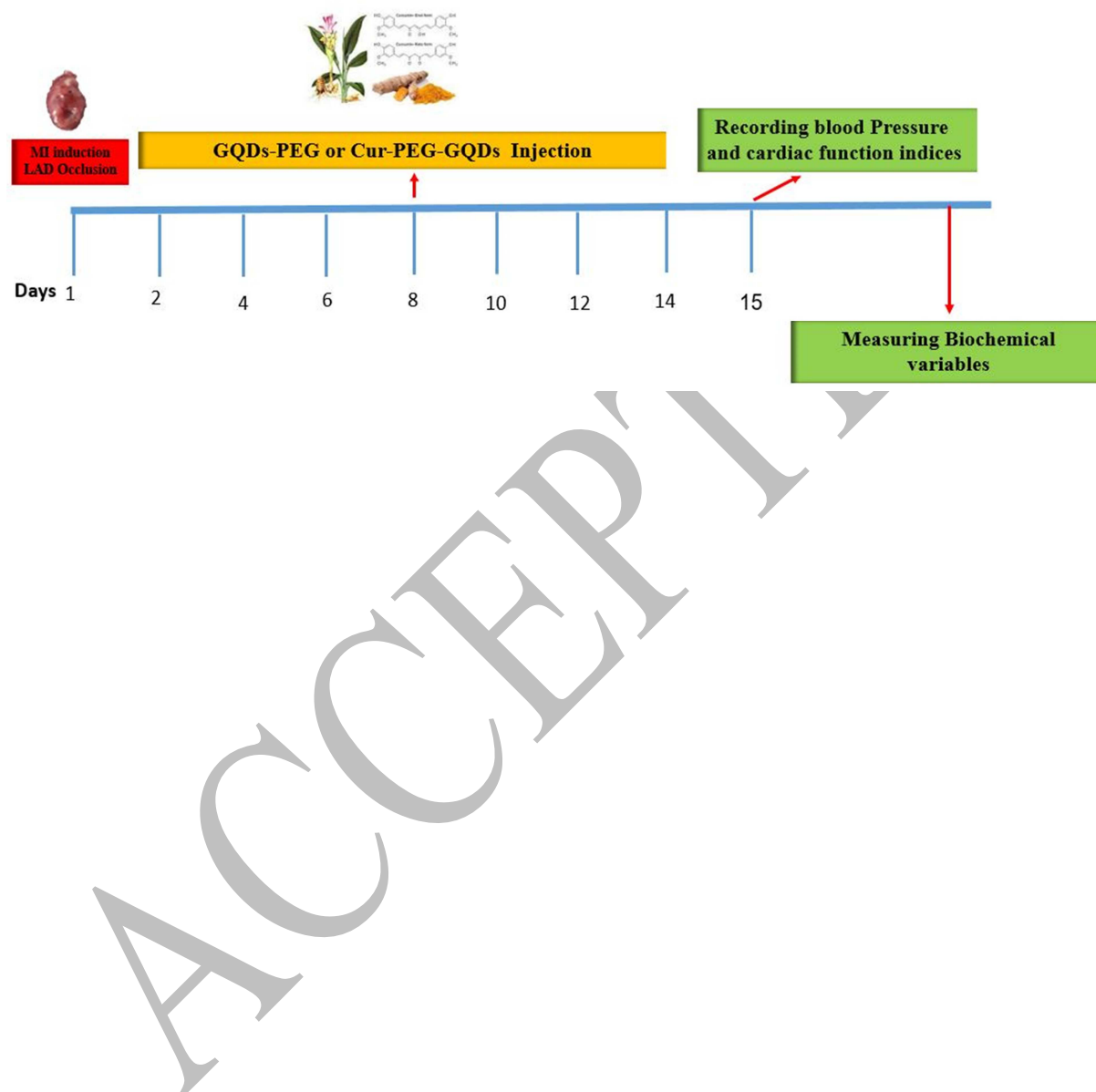
46. Santos-Parker JR, Strahler TR, Bassett CJ, Bispham NZ, Chonchol MB, Seals DR. Curcumin supplementation improves vascular endothelial function in healthy middle-aged and older adults by increasing nitric oxide bioavailability and reducing oxidative stress. *Aging (Albany NY)*. 2017;9:187-208. doi: 10.18632/aging.101149.

47. Ghosh SS, Gehr TWB, Ghosh S. Curcumin and Chronic Kidney Disease (CKD): Major Mode of Action through Stimulating Endogenous Intestinal Alkaline Phosphatase. *Molecules*. 2014;19:20139-56. doi: 10.3390/molecules191220139.

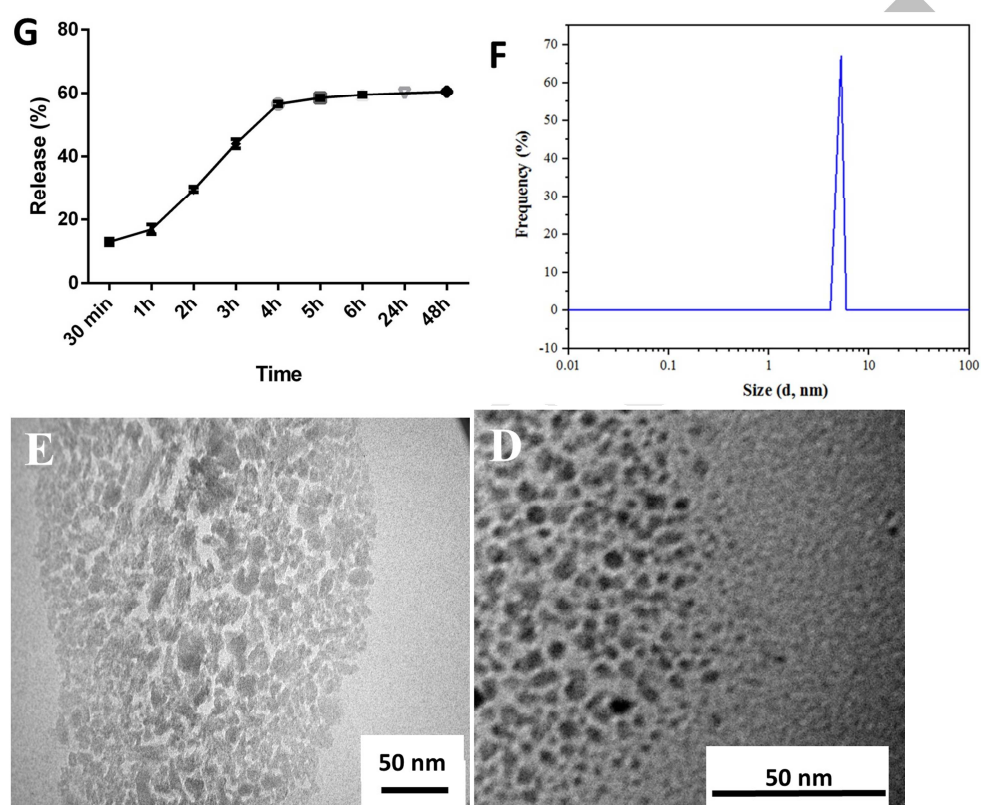
48. Sharma RA, Euden SA, Platton SL, Cooke DN, Shafayat A, Hewitt HR, et al. Phase I clinical trial of oral curcumin: biomarkers of systemic activity and compliance. *Clin Cancer Res*. 2004;10:6847–54. doi: 10.1158/1078-0432.CCR-04-0744.

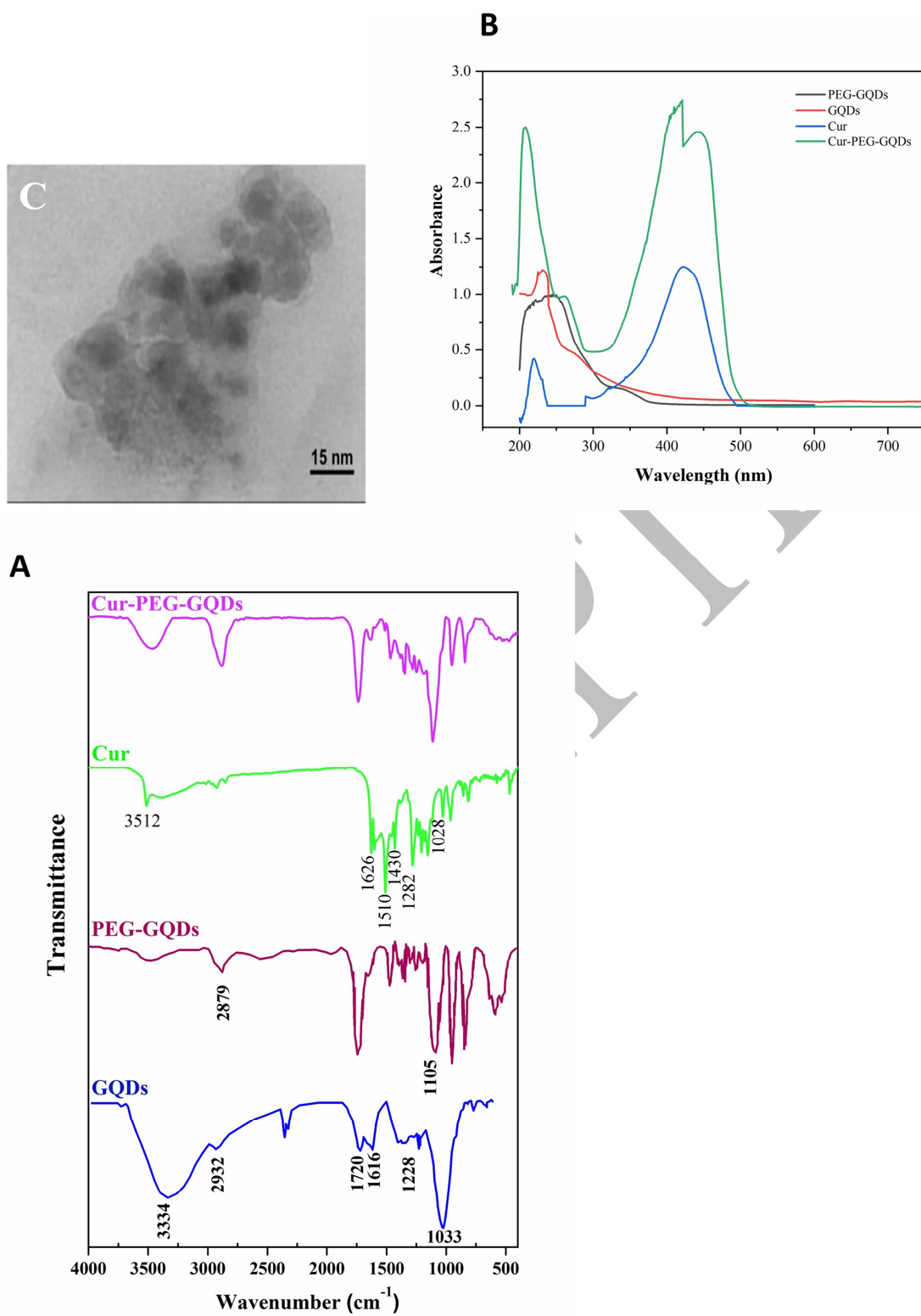
49. Lofthus DM, Stevens SR, Armstrong PW, Granger CB, Mahaffey KW. Pattern of liver enzyme elevations in acute ST-elevation myocardial infarction. *Coron Artery Dis*. 2012;23:22-30. doi: 10.1097/MCA.0b013e32834e4ef1.

**Fig. 1.** The schematic diagram shows the treatment protocol.



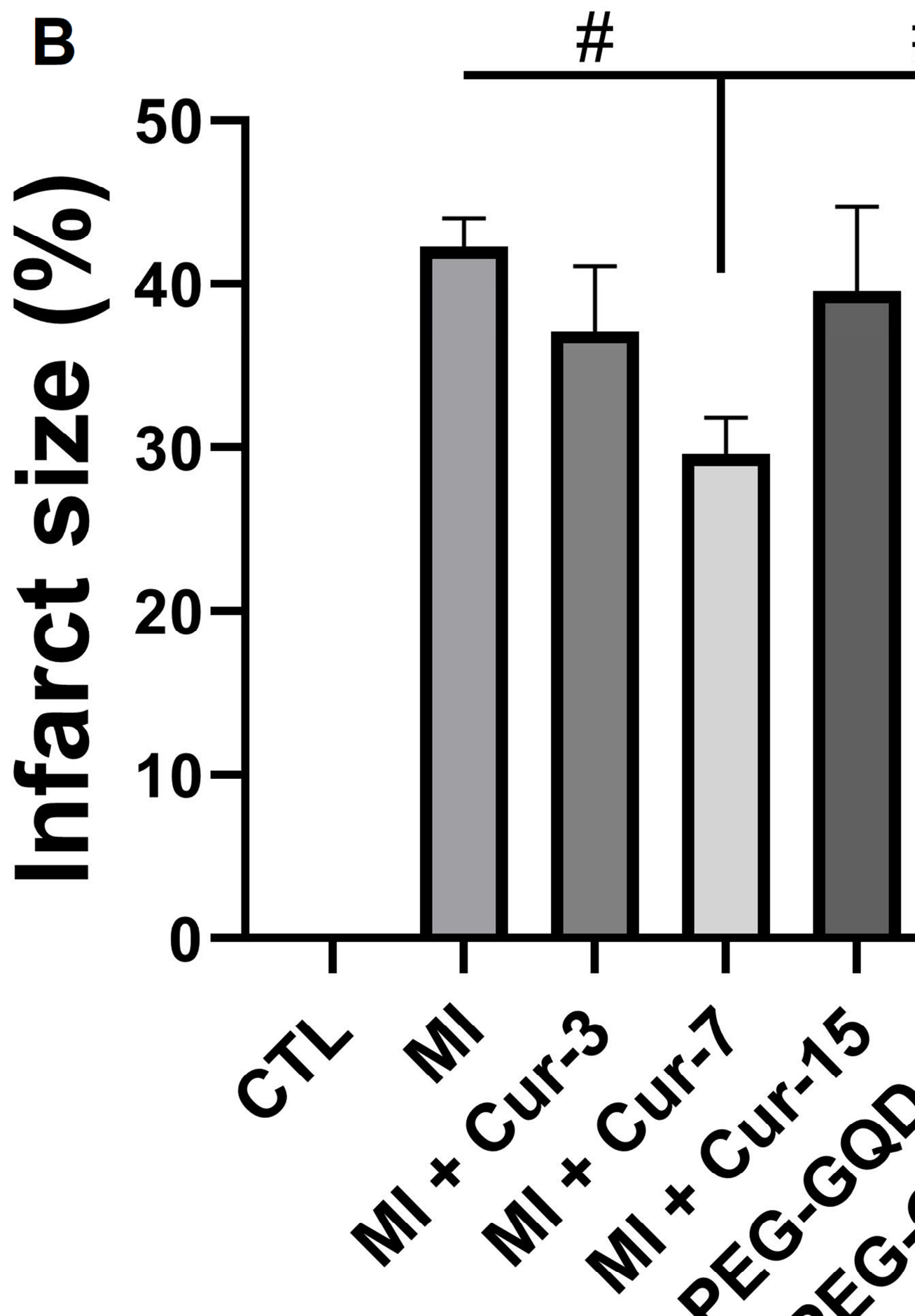
**Fig. 2.** Characterization of GQDs, PEG-GQDs, and Cur-PEG-GQDs. A: The FT-IR spectra of GQDs, PEG-GQDs, Cur, and Cur-PEG-GQDs. B: The UV-Vis spectra of GQDs, PEG-GQDs, Cur, and Cur-PEG-GQDs. TEM image of GQDs (C), PEG-GQD (D), and Cur-PEG-GQD (E). Particle size distribution of the as-prepared Cur-PEG-GQDs (F). In vitro release of curcumin from Cur-PEG-GQDs in PBS at pH 7.4.







**Fig. 3.** The infarct size decreased after two weeks of treatment with Cur-7, PEG-GQDs-10, Cur-PEG-GQDs-5, and Cur-PEG-GQDs-10. A: The heart transverse sections in one animal of each group with TTC staining. B: Quantification of infarct size. MI: myocardial infarction, Cur: Curcumin, PEG-GQDs: polyethylene glycol-graphene quantum dots, Cur-PEG-GQDs: Curcumin-graphene quantum dots-polyethylene glycol. #  $P < 0.05$  vs. MI.  $n = 5$  in each group.



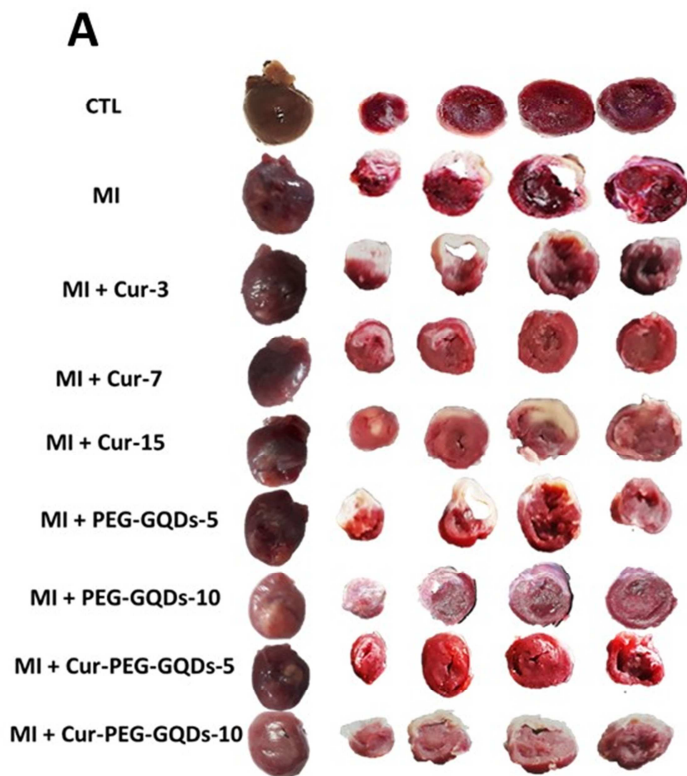


**Fig. 4.** The fibrosis decreased after two weeks of treatment with Cur-7, PEG-GQDs-10, Cur-PEG-GQDs-5, and Cur-PEG-GQDs-10. A: The percent of fibrosis in one animal of each group with Masson's trichrome. B: Quantification of fibrosis. MI: myocardial infarction, Cur: Curcumin, PEG-GQDs: graphene quantum dots-polyethylene glycol, Cur-PEG-GQDs: Curcumin-graphene quantum dots-polyethylene glycol. #  $P < 0.05$  vs. MI.  $n = 5$  in each group.

**Fibrotic area (%)**

**B**

30

20

10

0

#

#

CTL

MI

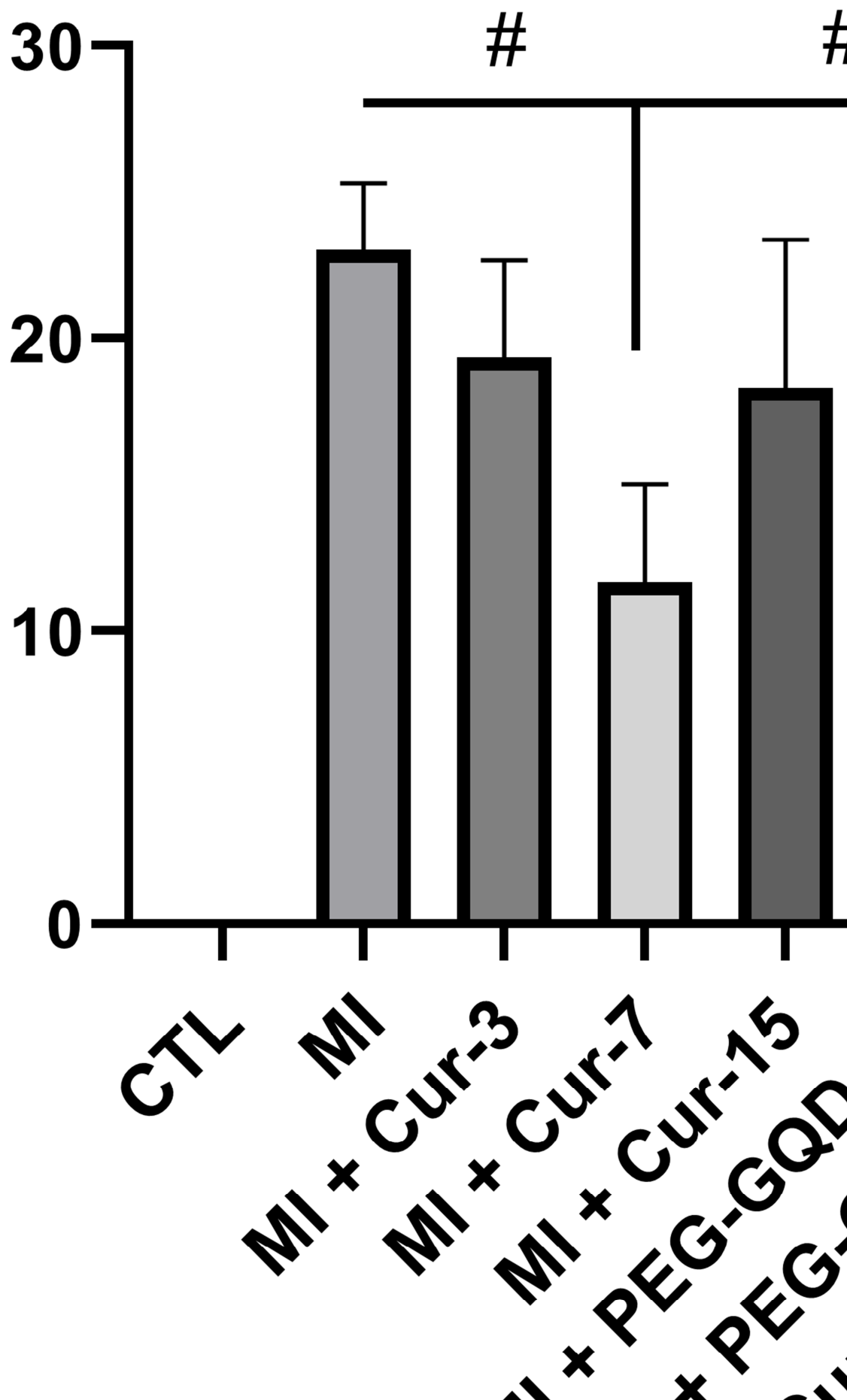
MI + Cur-3

MI + Cur-7

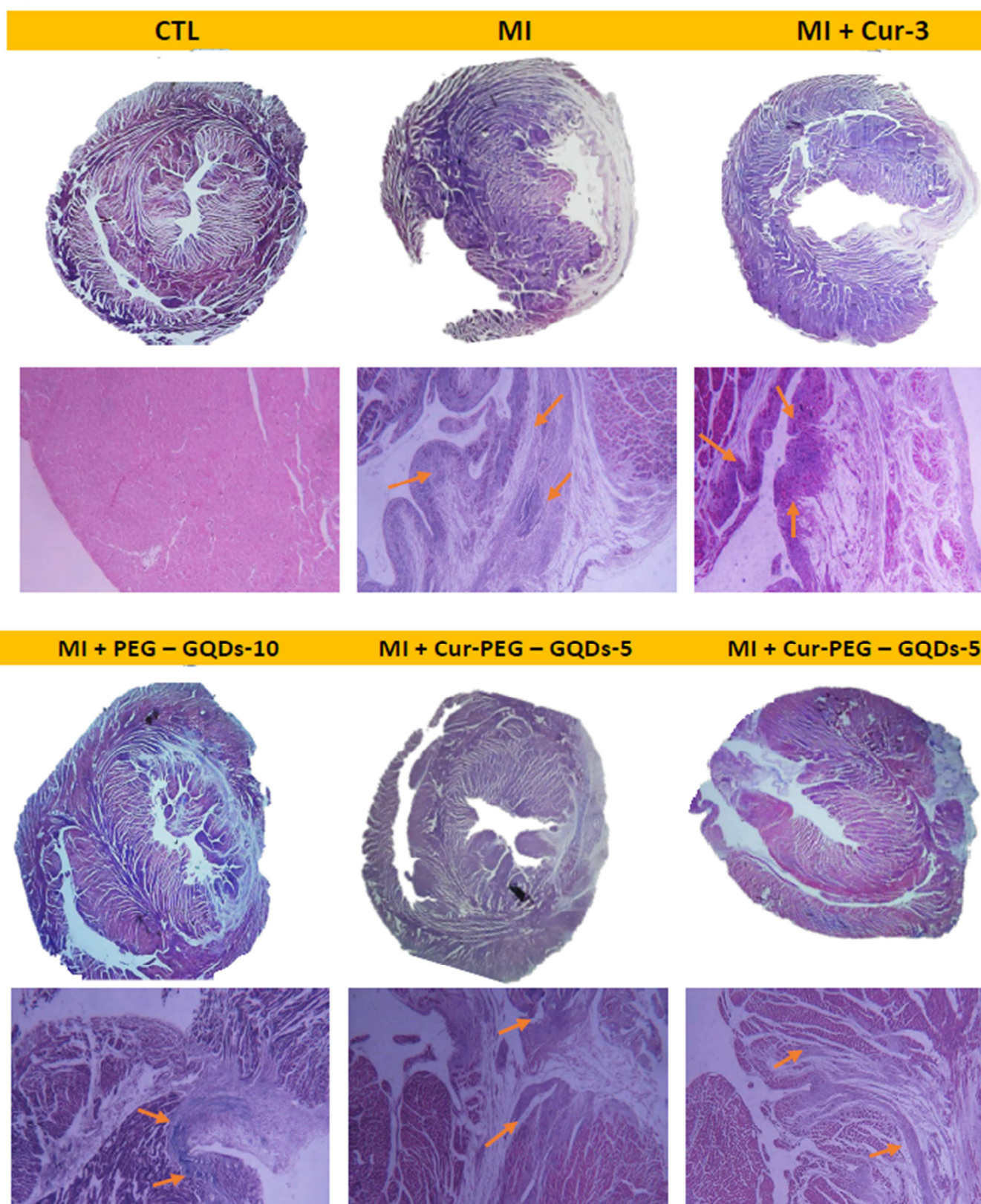
MI + Cur-15

MI + PEG-GQD

MI + PEG-GQD

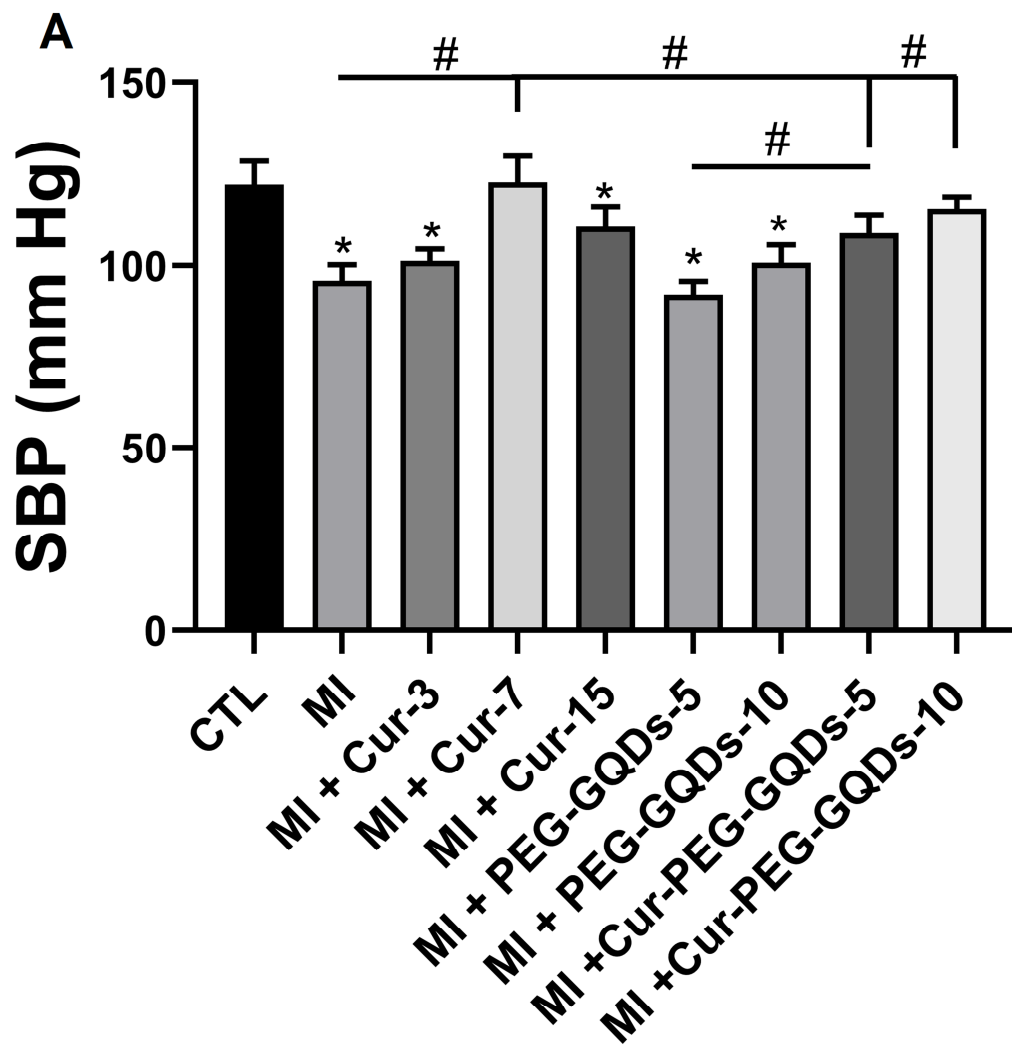


**A**

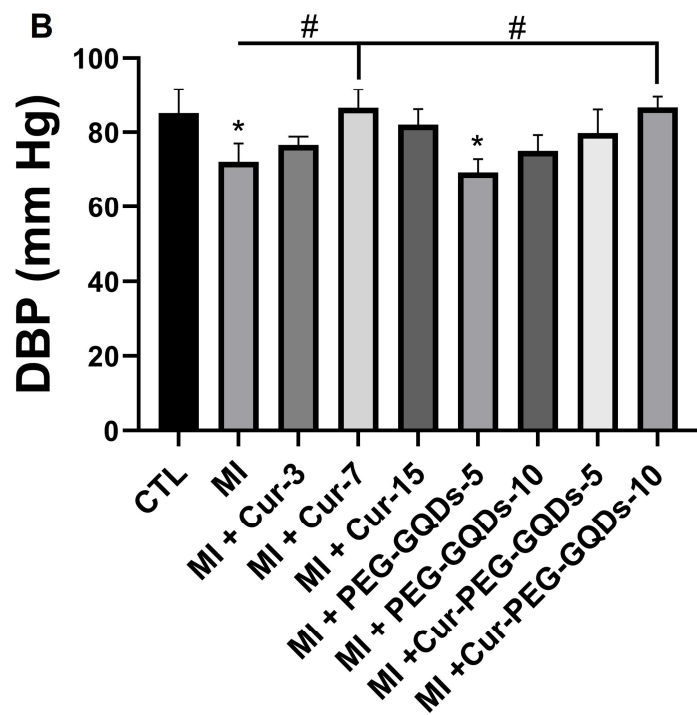


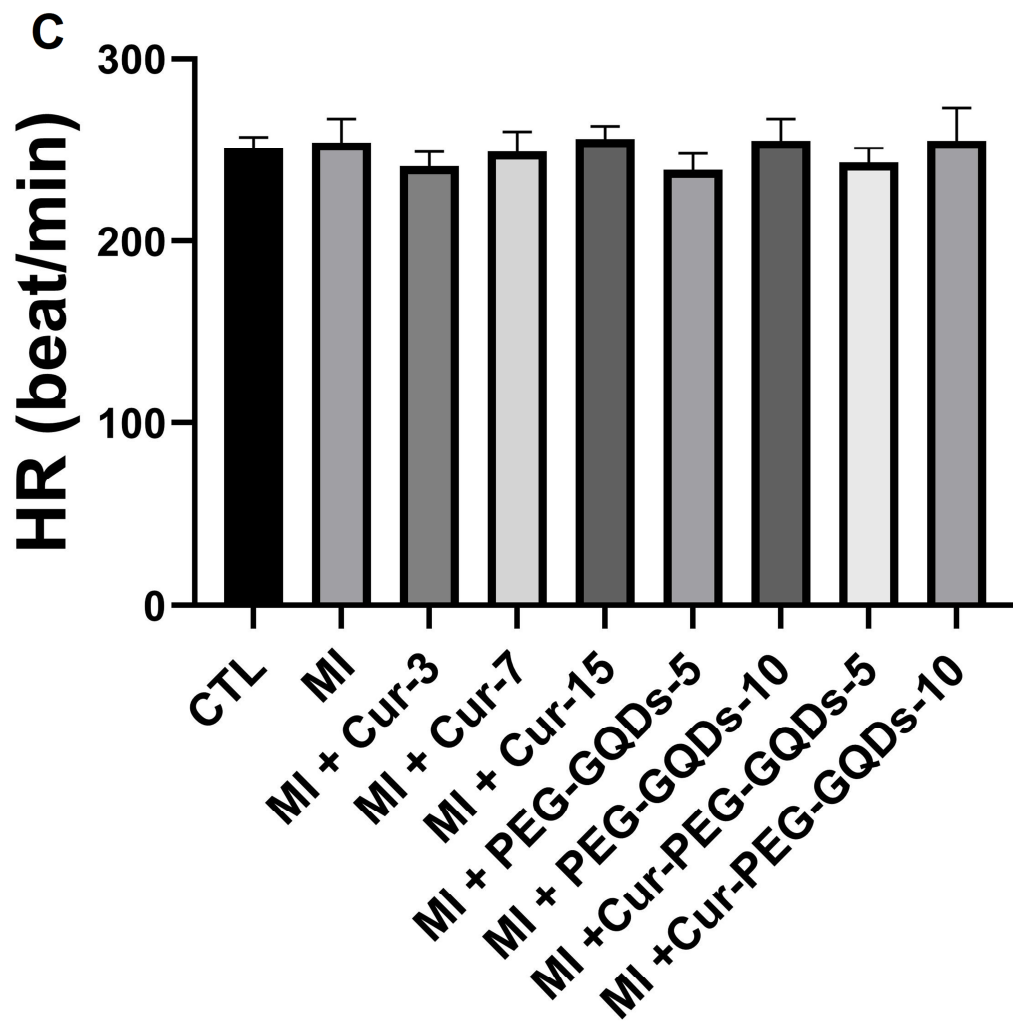
**Fig. 5.** Effects of two weeks treatment with Cur, PEG-GQDs, Cur-PEG-GQDs, and Cur-PEG-GQDs at different doses on A: SBP (systolic blood pressure), B: DBP (diastolic blood pressure), and C: HR (heart rate). \*  $P < 0.05$  vs. CTL; #  $P < 0.05$  vs. MI, and PEG-GQDs-5.  $n = 7$  in each group.

ACCEPTED



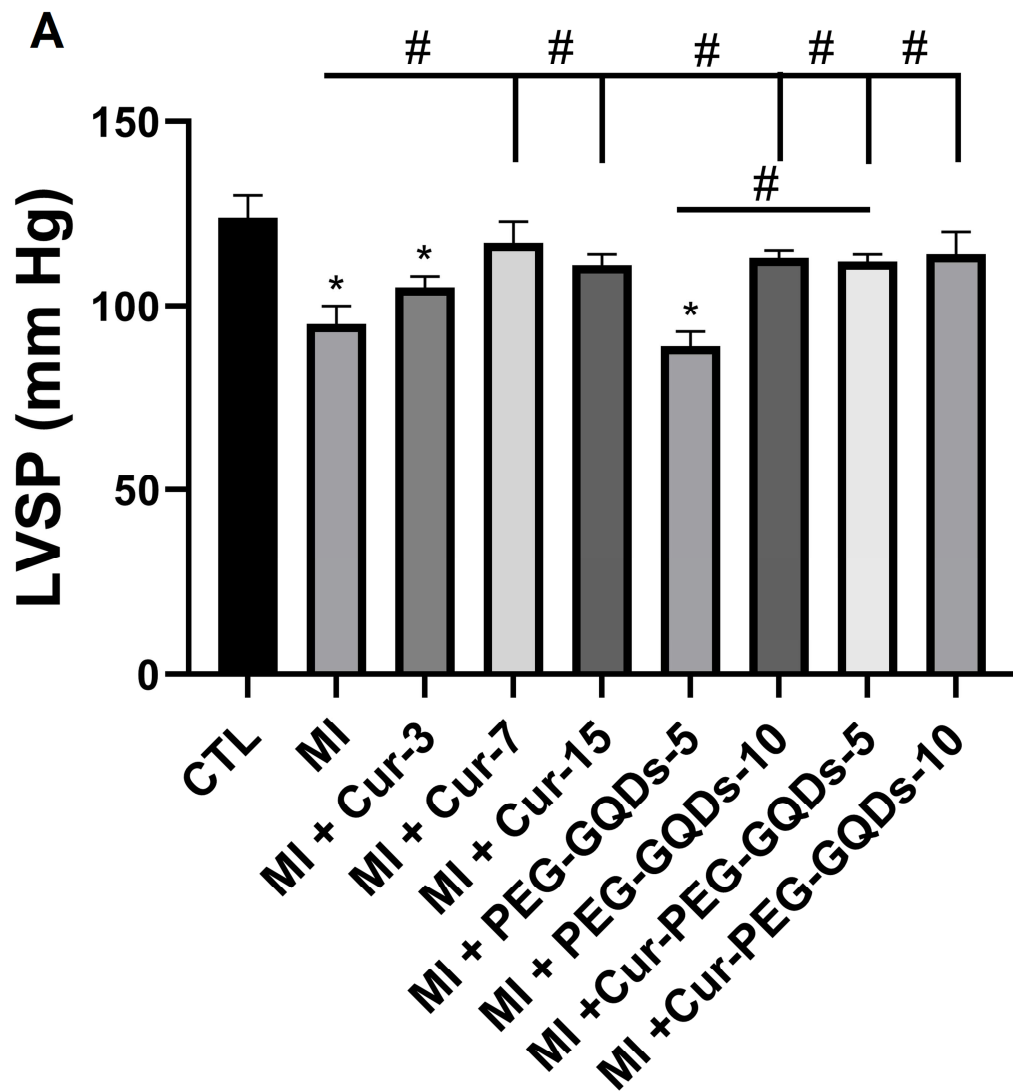


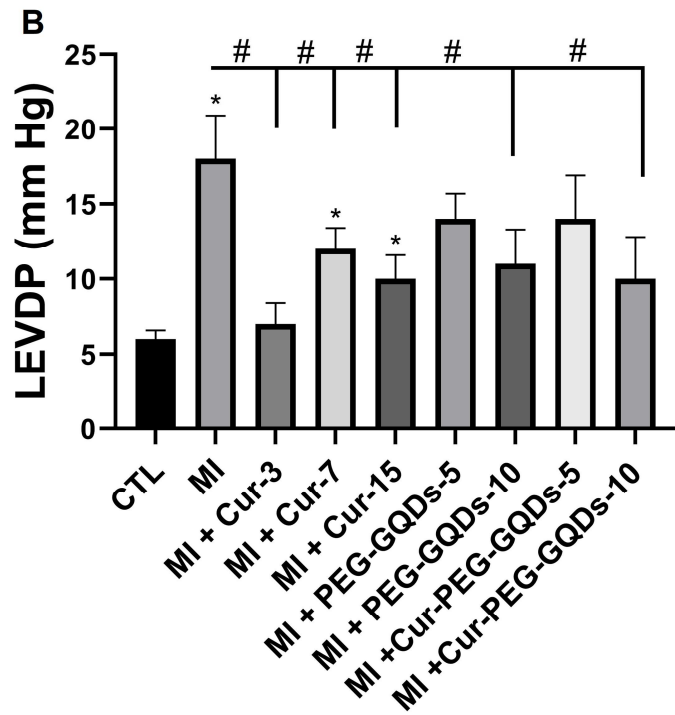


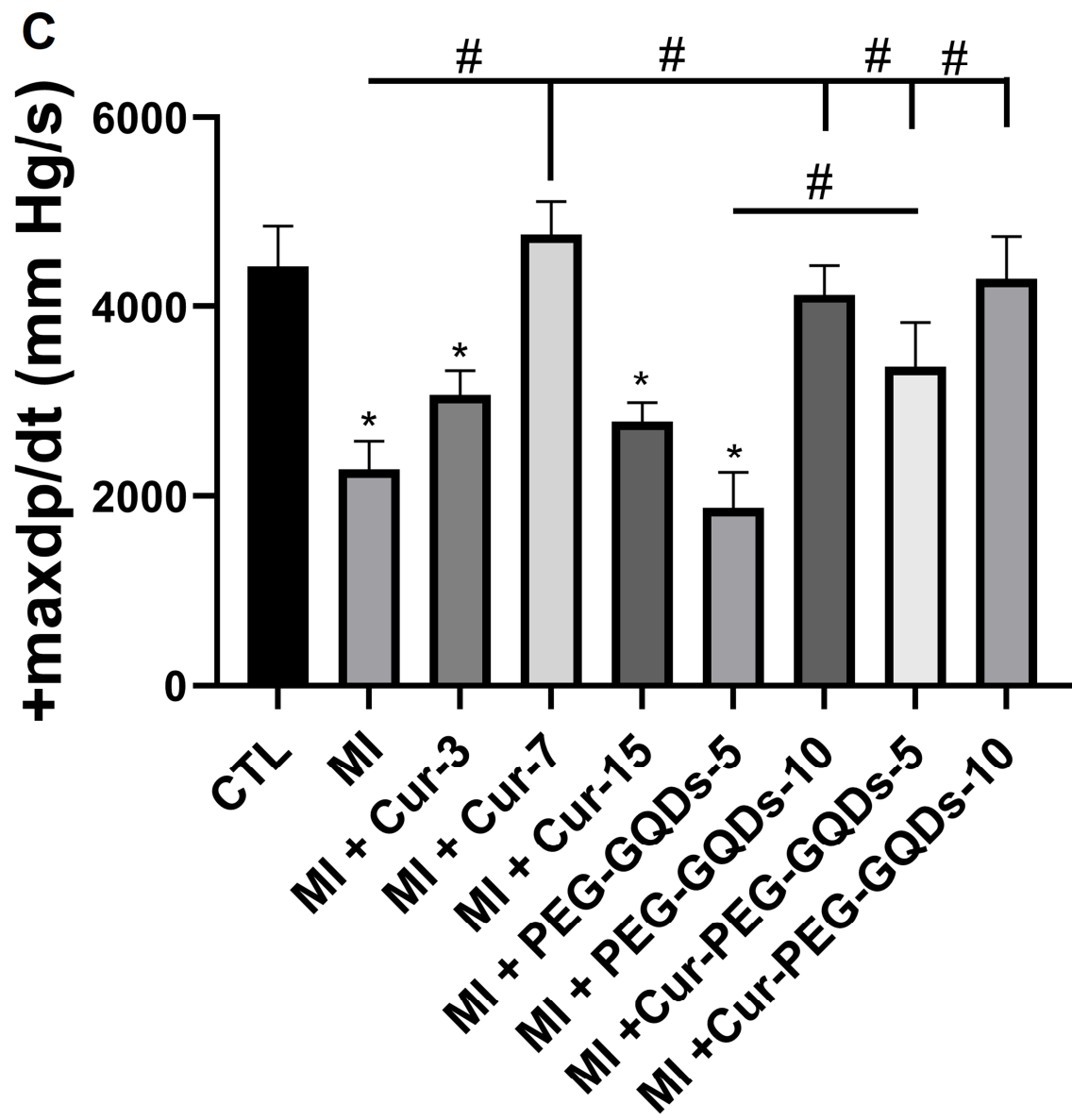


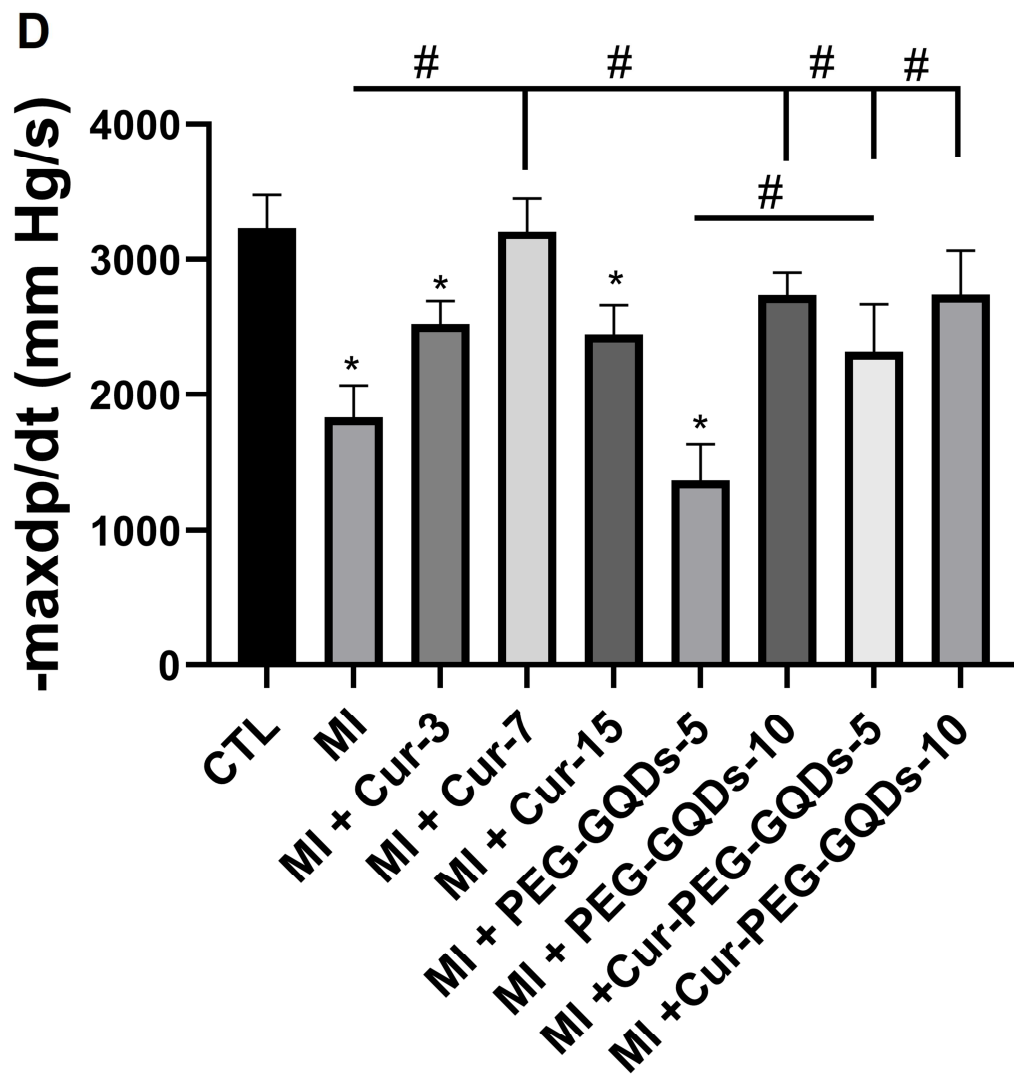
**Fig. 6.** Effects of two weeks treatment with Cur, PEG-GQDs and Cur-PEG-GQDs at different doses on A: LVSP (left ventricular systolic pressure): B: LVEDP (left ventricular end-diastolic pressure). C: +dp/dt max (maximum rate of increase in left ventricular pressure during systole), D: -dp/dt max (maximum rate of decrease in left ventricular pressure during diastole).\*  $P < 0.05$ , vs. CTL; #  $P < 0.05$  vs. MI and PEG-GQDs-5. n = 7 in each group.

ACCEPTED





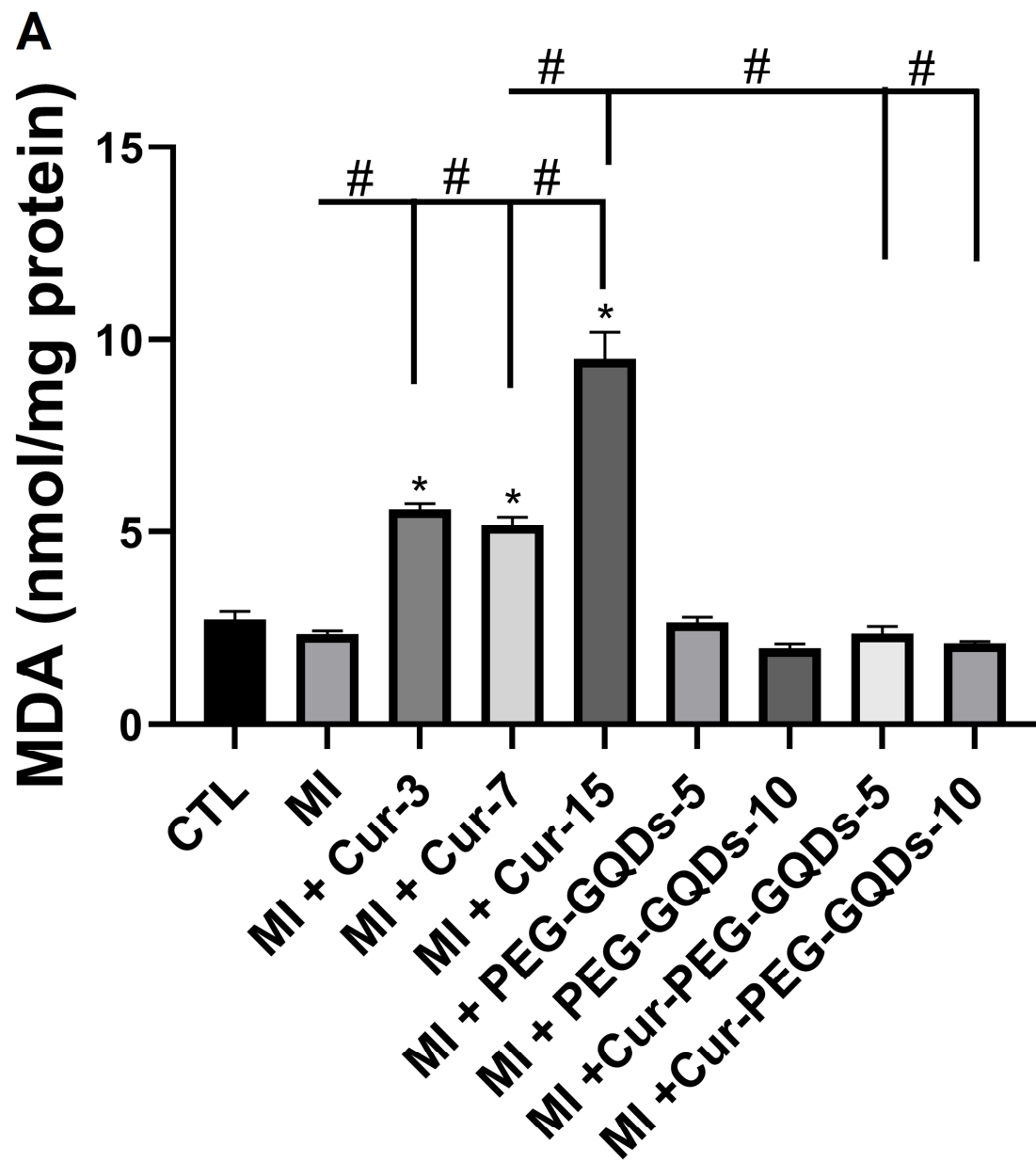


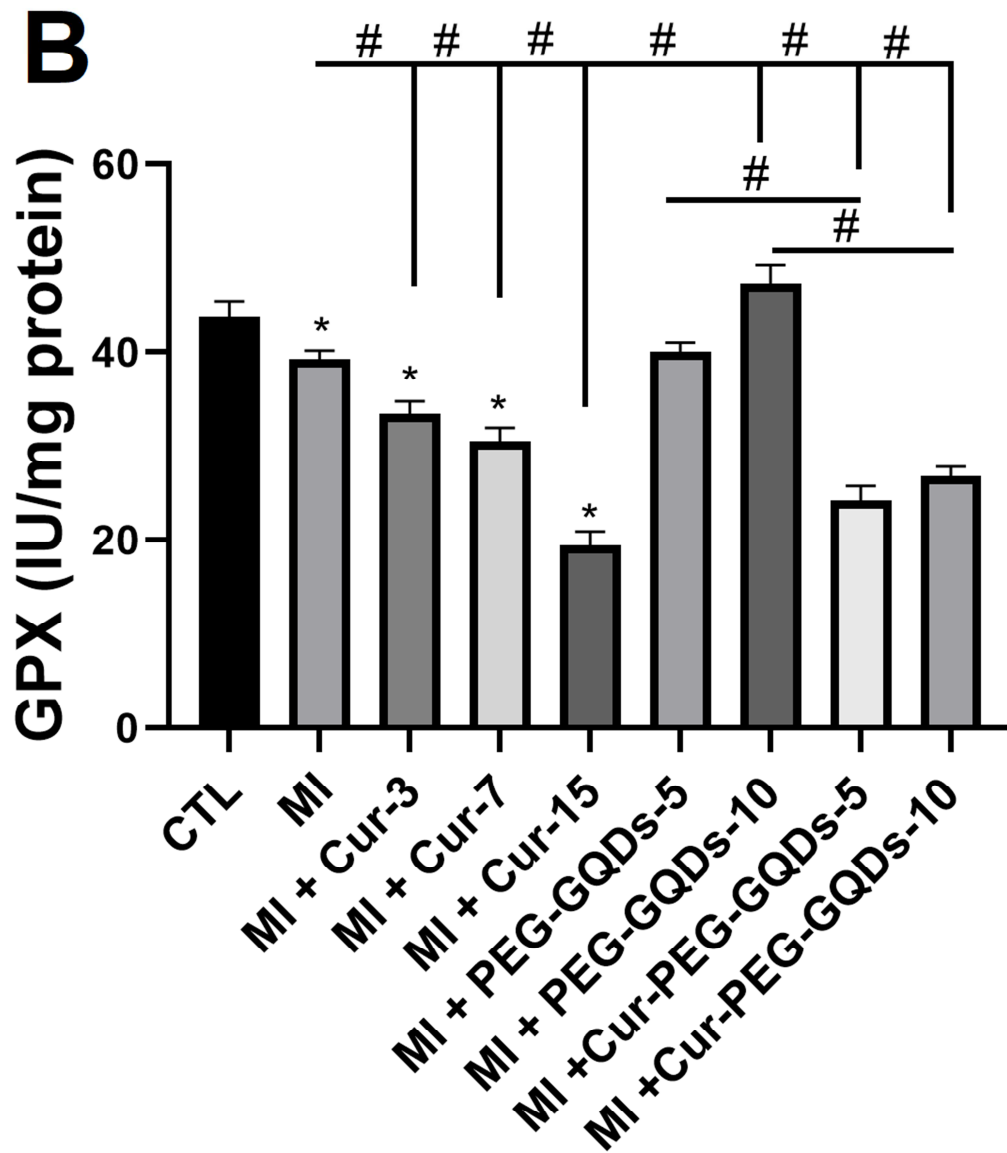


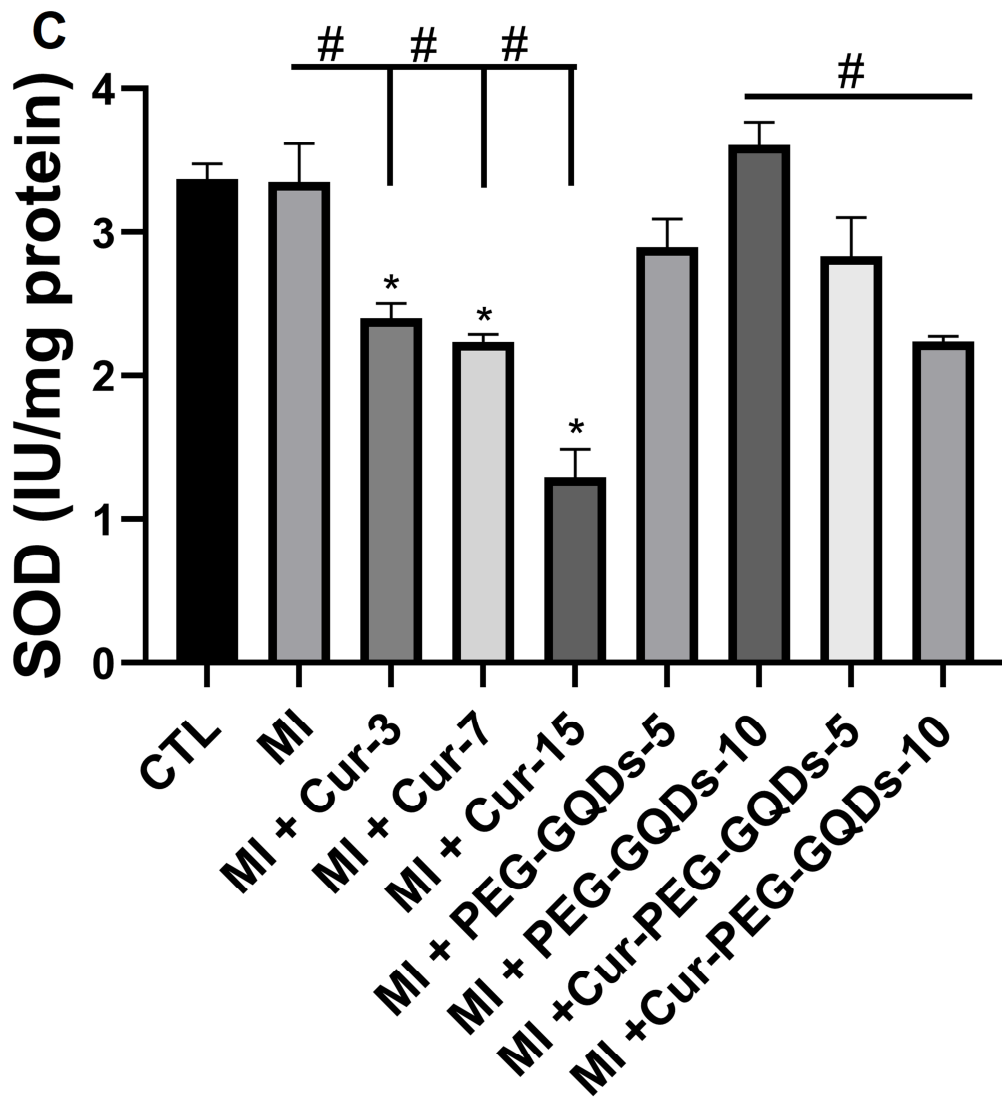
**Fig. 7.** Effects of two weeks treatment with Cur, PEG-GQDs, and Cur-PEG-GQDs at different doses on the heart levels of A: MDA (malondialdehyde), B: GPX (glutathione peroxidase), C: SOD (superoxide dismutase), and D: TAC (total antioxidant capacity). \*  $P < 0.05$  vs. CTL; #  $P < 0.05$  vs. MI, Cur-3 and 7, PEG-GQDs-5, and PEG-GQDs 10. n = 7 in each group.

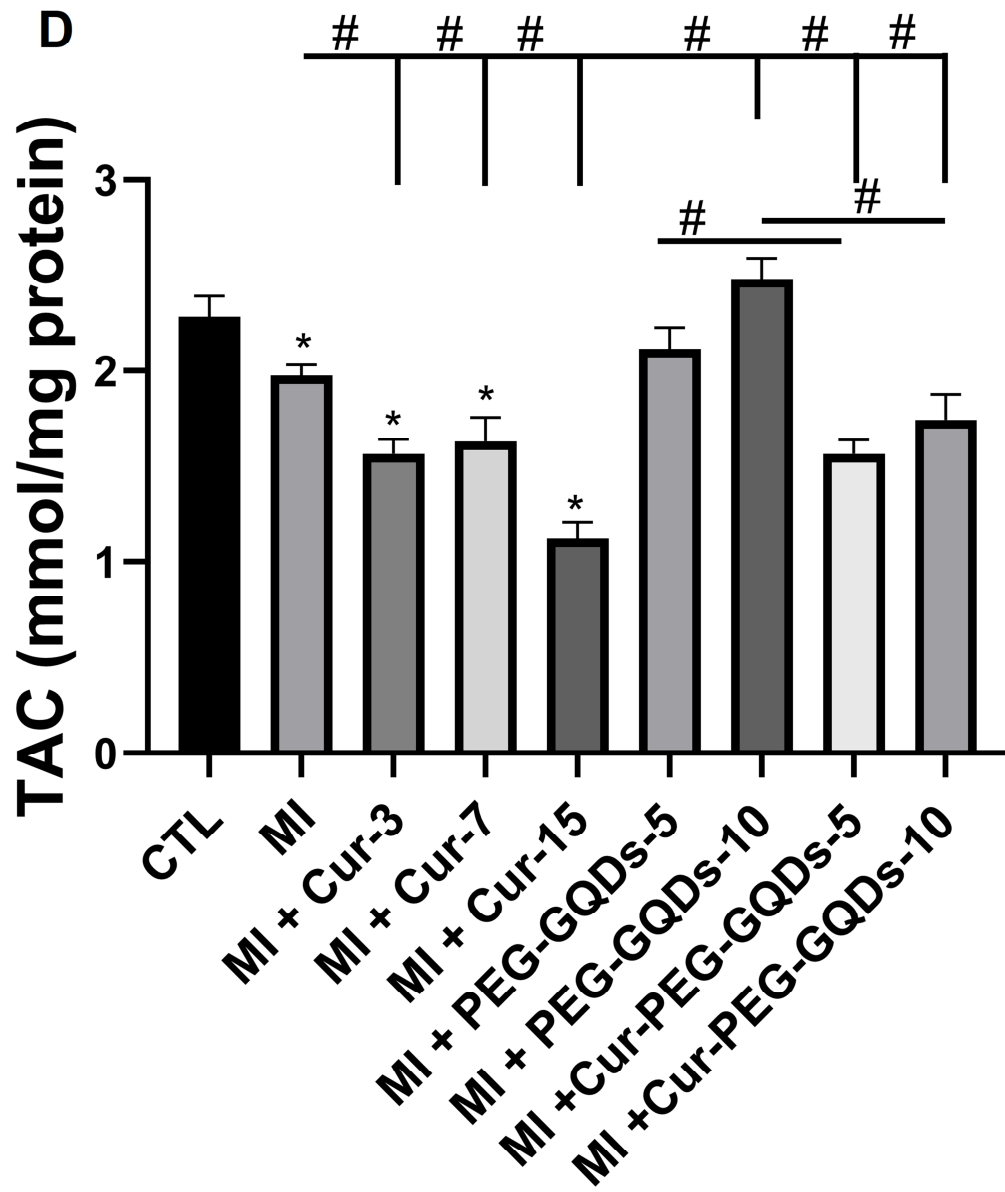
ACCEPTED





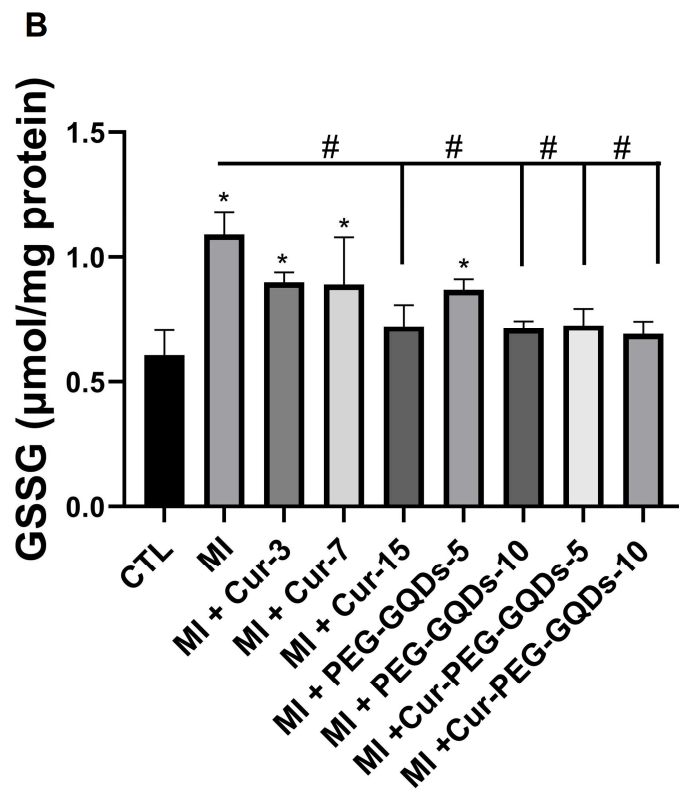
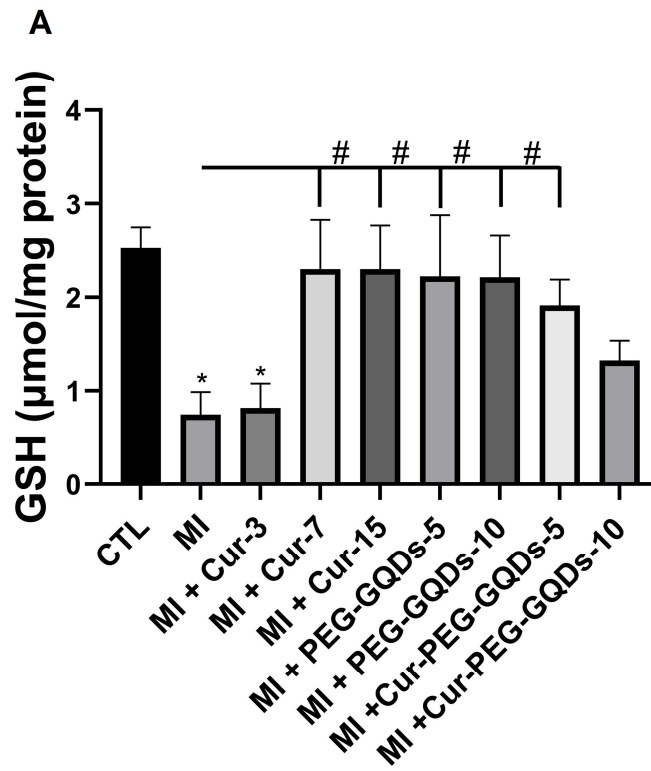


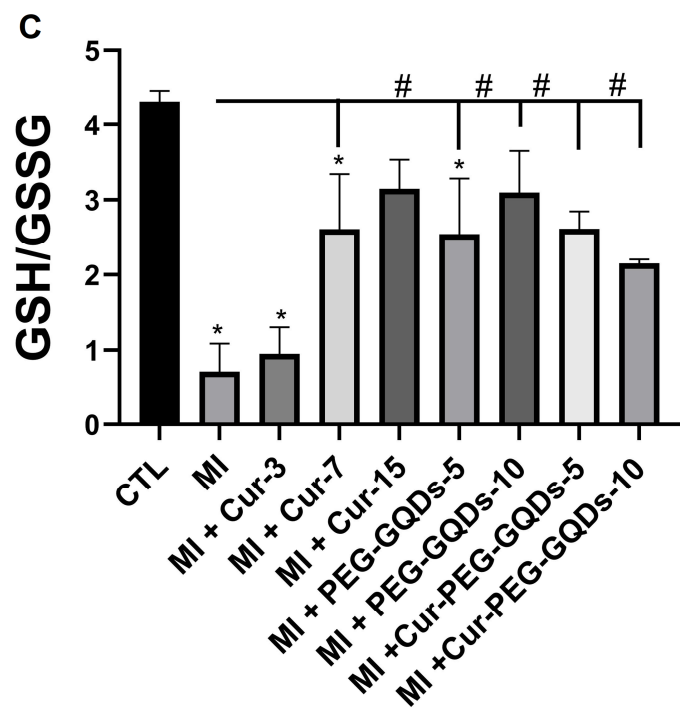




**Fig. 8.** Effects of two weeks treatment with Cur, PEG-GQDs, and Cur-PEG-GQDs at different doses on the heart levels of A: GSH, B: GSSG, C: the ratio of GSH/GSSG. \*  $P < 0.05$  vs. CTL; #  $P < 0.05$  vs. MI. n = 7 in each group.

ACCEPTED

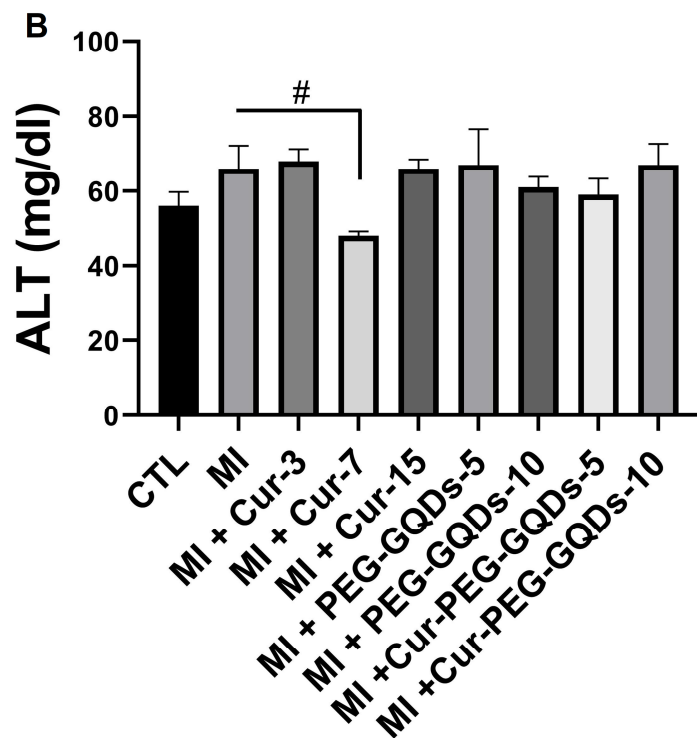
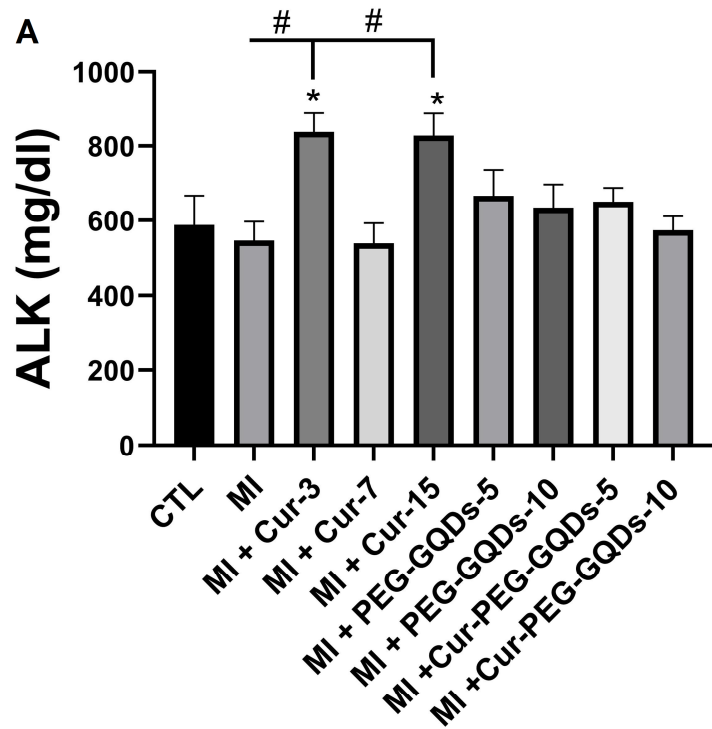




**Fig. 9.** Effects of two weeks of treatment with Cur, PEG-GQDs, and Cur-PEG-GQDs at different doses on the serum levels of A: ALP (alkaline phosphatase), B: ALT (alanine aminotransferase), and C: AST (aspartate aminotransferase). \*  $P < 0.05$  vs. CTL; #  $P < 0.05$  vs. MI. n = 7 in each group.

ACCEPTED





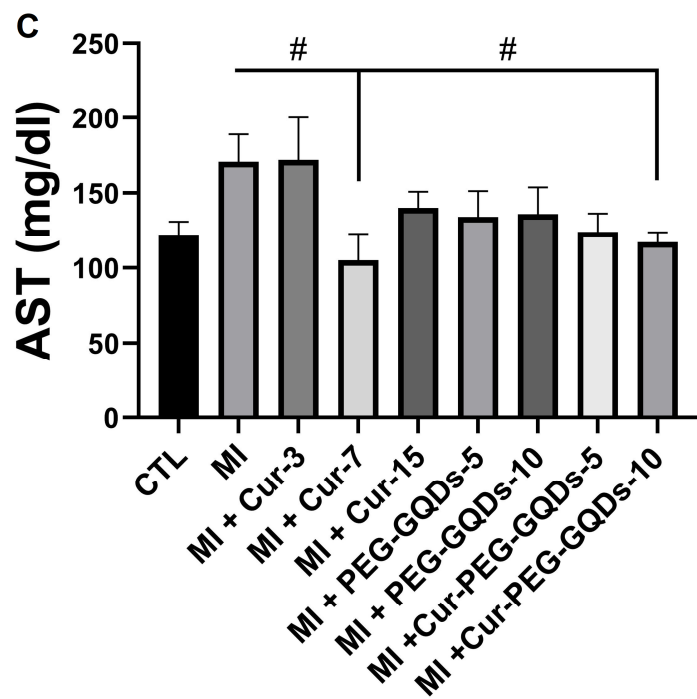
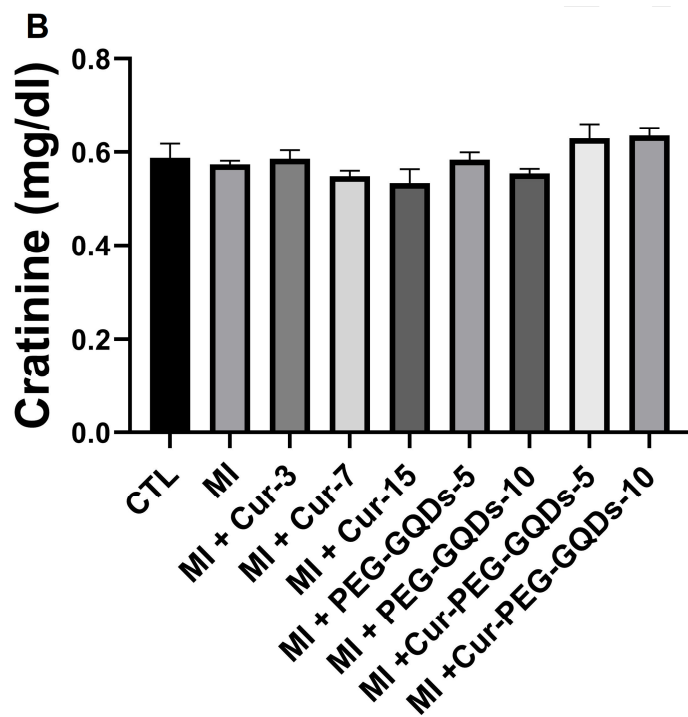
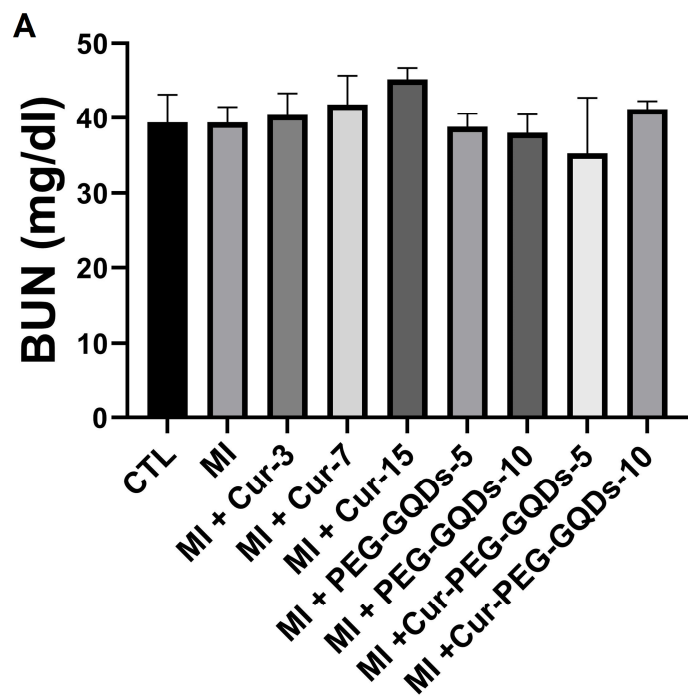


**Fig. 10.** Effects of two weeks of treatment with Cur, PEG-GQDs, and Cur-PEG-GQDs at different doses on the serum levels of urea (A), and creatinine (B), in the studied groups. n = 7 in each group.

ACCEPTED



<b>Variables</b> <b>Groups</b>	<b>BW (GR)</b>	<b>HW/BW</b> <b>(MG/G)</b>	<b>LVW/BW</b> <b>(MG/G)</b>	<b>LW/BW</b> <b>(MG/G)</b>
<b>CTL</b>	239 ± 14.70	2.8 ± 0.07	2.2 ± 0.049	5.5 ± 0.19
<b>MI</b>	242 ± 8.25	2.97 ± 0.06	2.27 ± 0.09	6.18 ± 0.36
<b>MI+CU 3</b>	232 ± 10	2.83 ± 0.09	2.26 ± 0.11	5.82 ± 0.26
<b>MI+CU 7</b>	231 ± 7.90	3.05 ± 0.08	2.28 ± 0.07	6.01 ± 0.24
<b>MI+CU 15</b>	224 ± 9.09	3.03 ± 0.16	2.18 ± 0.15	5.71 ± 0.27

**Table 1.** Bodyweight and left ventricular, and lung weight/ body weight ratios in the studied groups

<b>MI+PEG-GQDS 5</b>	246 ± 7.95	2.76 ± 0.10	2.09 ± 0.06	5.43 ± 0.29
<b>MI+PEG-GQDS 10</b>	232 ± 7.24	2.92 ± 12	2.08 ± 10	5.64 ± 0.14
<b>MI+CUR-PEG-GQDS 5</b>	253 ± 4.51	2.79 ± 0.06	2.24 ± 0.07	5.52 ± 0.24 <sup>#</sup>
<b>MI+CUR-PEG-GQDS 10</b>	232 ± 6.02	2.96 ± 0.11	2.30 ± 0.05	5.30 ± 0.28 <sup>#</sup>

**LVW**: left ventricle + septum weight, **BW**: bodyweight, **LW**: lung weight, **MI**: myocardial infarction, **Cur**: curcumin, **PEG-GQDs**: polyethylene glycol-graphene quantum dots, **Cur-PEG-GQDs**: Curcumin-polyethylene glycol-graphene quantum dots. Values are Mean ± SEM. #  $P < 0.05$  vs. MI group.  $n = 7$  in each group.